Received: 6 September 2022 | Revised: 19 January 2023 | Accepted: 6 February 2023

DOI: 10.1002/pld3.486

ORIGINAL RESEARCH

Identification of new potential downstream transcriptional targets of the strigolactone pathway including glucosinolate biosynthesis

Alicia M. Hellens[1,2] | Tinashe G. Chabikwa[1,3†] | Franziska Fichtner[1,2,4] | Philip B. Brewer[1,2,5] | Christine A. Beveridge[1,2]

[1]School of Biological Sciences, University of Queensland, St. Lucia, Queensland, Australia

[2]ARC Centre for Plant Success in Nature and Agriculture, The University of Queensland, St Lucia, Queensland, Australia

[3]QIMR Berghofer Medical Research Institute, Brisbane, Queensland, Australia

[4]Institute for Plant Biochemistry, Heinrich Heine University, Düsseldorf, Germany

[5]School of Agriculture, Food and Wine, The University of Adelaide, Glen Osmond, South Australia, Australia

Correspondence
Alicia M. Hellens and Christine A. Beveridge, School of Biological Sciences, University of Queensland, St. Lucia, QLD 4072, Australia.
Email: a.hellens@uq.net.au and c.beveridge@uq.edu.au

Funding information
Department of Education and Training | ARC | Australian Research Council Centre of Excellence for Plant Success in Nature and Agriculture (ARC CoE for Plant Success in Nature and Agriculture), Grant/Award Number: CE200100015; Australian Laureate Fellowship, Grant/Award Number: FL180100139; Commonwealth Scientific and Industrial Research Organization; Australian Research Council, Grant/Award Number: FT180100081

Abstract

Strigolactones regulate shoot branching and many aspects of plant growth, development, and allelopathy. Strigolactones are often discussed alongside auxin because they work together to inhibit shoot branching. However, the roles and mechanisms of strigolactones and how they act independently of auxin are still elusive. Additionally, there is still much in general to be discovered about the network of molecular regulators and their interactions in response to strigolactones. Here, we conducted an experiment in Arabidopsis with physiological treatments and strigolactone mutants to determine transcriptional pathways associated with strigolactones. The three physiological treatments included shoot tip removal with and without auxin treatment and treatment of intact plants with the auxin transport inhibitor, *N*-1-naphthylphthalamic acid (NPA). We identified the glucosinolate biosynthesis pathway as being upregulated across strigolactone mutants indicating strigolactone–glucosinolate crosstalk. Additionally, strigolactone application cannot restore the highly branched phenotype observed in glucosinolate biosynthesis mutants, placing glucosinolate biosynthesis downstream of strigolactone biosynthesis. Oxidative stress genes were enriched across the experiment suggesting that this process is mediated through multiple hormones. Here, we also provide evidence supporting non-auxin-mediated, negative feedback on strigolactone biosynthesis. Increases in strigolactone biosynthesis gene expression seen in strigolactone mutants could not be fully restored by auxin. By contrast, auxin could fully restore auxin-responsive gene expression increases, but not sugar signaling-related gene expression. Our data also point to alternative roles of the strigolactone biosynthesis genes and potential new signaling functions of strigolactone precursors.

In this study, we identify a strigolactone-specific regulation of glucosinolate biosynthesis genes indicating that the two are linked and may work together in regulating

[†]The author died prior to the submission of this paper.

stress and shoot ranching responses in Arabidopsis. Additionally, we provide evidence for non-auxinmediated feedback on strigolactone biosynthesis and discuss this in the context of sugar signaling.

KEYWORDS
Arabidopsis thaliana, auxin, flavonoids, glucosinolates, strigolactones, transcriptomic

1 | INTRODUCTION

Strigolactones (SLs) are a group of recently discovered plant hormones that play a role in many aspects of plant growth and development (reviewed in Brewer et al., 2013). SLs were first associated with, and subsequently named after, the parasitic weed of genus *Striga* or witchweed (Cook et al., 1972). Exogenous SLs exuded from plant roots in poor nutrient conditions induce *Striga* germination and provide beneficial symbiotic interactions with arbuscular mycorrhizal (AM) fungi (Bouwmeester et al., 2007). In 2008, SLs were identified as plant hormones that have a role in signaling, particularly in the inhibition of shoot branching or axillary bud outgrowth (Gomez-Roldan et al., 2008; Umehara et al., 2008). SLs have since been intricately studied and are clearly an important aspect of plant growth and development because they act in networks with most other plant hormones and are impacted by nutrient and signaling pathways (recent reviews: Barbier et al., 2019; Bürger & Chory, 2020; Faizan et al., 2020; Kelly et al., 2023; Saeed et al., 2017).

In the past decade or so, much of the SL biosynthetic and signaling pathway has been elucidated (reviewed in Yoneyama & Brewer, 2021). In Arabidopsis, bioactive SLs are synthesized from β-carotene through consecutive reactions catalyzed by β-carotene isomerase DWARF27 (D27); CAROTENOID CLEAVAGE DIOXYGENASE7 and 8 (CCD7 and CCD8), encoded by *MORE AXILLARY GROWTH3* and *4* (*MAX3* and *MAX4*) genes, respectively; *MAX1*, which encodes a cytochrome P450 CYP711A1; a carlactonoic acid methyltransferase (CLAMT); and LATERAL BRANCHING OXIDOREDUCTASE (LBO) (Abe et al., 2014; Alder et al., 2012; Brewer et al., 2016; Mashiguchi et al., 2022; Seto et al., 2014). More recently, SL has been demonstrated to be catabolized by carboxylesterase enzyme, CXE15 (Xu et al., 2021). SL perception and signaling involve the F-box protein MORE AXILLARY GROWTH2 (MAX2) and the α/β-fold hydrolase DWARF14 (D14), which form a complex that binds SUPPRESSOR OF MAX2 1-LIKE target proteins SMXL6, SMXL7, and SMXL8 (also known as DWARF53 [D53]) for degradation to release downstream genes from inhibition and allowing SL responsiveness (Arite et al., 2009; Chevalier et al., 2014; Ishikawa et al., 2005; Soundappan et al., 2015; Stirnberg et al., 2007; Wang et al., 2015). MAX2 is also involved in karrikin signaling (Nelson et al., 2011).

Genes that show similar expression patterns, or are co-expressed, have the potential to encode proteins with a related function, or which participate in similar biological processes (Eisen et al., 1998; Marcotte et al., 1999). Some aspects of the SL pathway are co-regulated, such as SL biosynthesis genes *MAX3* and *MAX4*. This knowledge allowed for the discovery of other SL biosynthesis components *LBO* and the Arabidopsis ortholog of rice *D27*, as they were both found to be upregulated in other SL mutants in a similar manner to the previously confirmed SL biosynthesis genes *MAX3* and *MAX4* (Brewer et al., 2016; Waters, Brewer, et al., 2012). After identifying the co-regulated expression patterns, mutants for *lbo* and *d27* were identified and shown to have enhanced branching and ultimately to act on the SL pathway. Given the success of this approach in identifying new SL biosynthesis genes (Brewer et al., 2016; Waters, Brewer, et al., 2012), we postulate that additional aspects of the SL regulatory network can be deciphered by interpreting co-regulated genes.

Increased SL biosynthesis gene expression in SL-deficient mutants is indicative of a negative feedback loop that has long been associated with the plant hormone auxin (Hayward et al., 2009; Ligerot et al., 2017). Auxin is one of the most well-researched plant hormones. Auxin promotes SL biosynthesis gene expression (Yoneyama & Brewer, 2021) and, in turn, SL inhibits auxin biosynthesis, transport, and canalization (Crawford et al., 2010; Ligerot et al., 2017; Shinohara et al., 2013; Zhang et al., 2020). Apically derived auxin upregulates the SL biosynthesis genes *MAX3*, *MAX4*, *LBO*, and *D27* (Bennett et al., 2006; Brewer et al., 2016; Hayward et al., 2009; Shen et al., 2012; Waters, Brewer, et al., 2012). MAX2- and D14-dependent SL perception, in turn, inhibits auxin transport (Bennett et al., 2006; Crawford et al., 2010; Ligerot et al., 2017). In the SL-deficient mutants, *max3* and *max4*, MAX2-mediated inhibition of auxin transport does not occur because of lack of SL signal perception and transduction. High endogenous levels of auxin in SL mutants (Beveridge, 2000) indicate that auxin may contribute to negative feedback, resulting in increased SL biosynthesis gene expression in SL-deficient mutants (Brewer et al., 2009; Foo et al., 2005; Hayward et al., 2009; Waters, Brewer, et al., 2012). However, the magnitude of upregulation of *MAX3* and *MAX4* gene expression in response to exogenous auxin is much less than the increase observed in SL mutants (Bennett et al., 2006; Hayward et al., 2009). This indicates that some other factors may be involved. Additionally, auxin is not the only contributor to SL-mediated responses, and non-auxin signals also regulate aspects of plant development (Bainbridge et al., 2005; Barbier et al., 2019; Faizan et al., 2020). We therefore hypothesize that there is also a non-auxin-mediated feedback on SL biosynthesis.

Sucrose has recently re-emerged as a major player in apical dominance (Barbier, Lunn, & Beveridge, 2015; Mason et al., 2014) and may act via a number of signaling pathways. Trehalose 6-phosphate (T6P) is a sucrose-specific signaling molecule, with T6P levels being strongly correlated with sucrose levels in plants (Fichtner & Lunn, 2021). T6P levels strongly correlate with bud outgrowth in pea (Fichtner

et al., 2017). Additionally, transgenic Arabidopsis plants with increased levels of T6P show increased branching (Fichtner et al., 2021), implicating T6P in the regulation of lateral bud outgrowth. Sucrose can be broken down into glucose and fructose. The enzyme HEXOKINASE (HXK) is the first enzyme in glycolysis that adds a phosphate to glucose to form glucose 6-phosphate. In Arabidopsis, the HXK1-deficient mutant, *gin2*, has reduced rosette branching and also shows increased *MAX2* expression (Barbier et al., 2021). Interestingly, sucrose antagonizes the SL-induced repression of shoot branching (or tillering) in rice, partially by inhibiting *OsMAX2* gene expression and by antagonizing the SL-mediated degradation of D53 (Bertheloot et al., 2020; Patil et al., 2021).

To determine novel processes co-regulated with SLs, and to investigate auxin-related feedback, we conducted a large-scale, genome-wide gene expression study. This study was previously used to discover *LBO*, which is co-expressed with *MAX3* and *MAX4* (Brewer et al., 2016). We revisited this prior data set to extrapolate more information. Recent progress in transcriptome analysis has investigated the response to SL, and SL mutants separately (Kumar et al., 2019; Wang et al., 2020). Our study compared SL-modifying physiological treatments with SL mutants. Mutant genotypes combined with physiological treatments in wild type (WT) allowed us to determine processes that are differentially regulated and co-regulated by SL independent of auxin. We identified differentially expressed and co-expressed genes in SL biosynthesis (*max1*, *max3*) and signaling (*max2*), mutants, as well as in WT Arabidopsis plants in response to decapitation with, and without the addition of auxin, indole-3-acetic acid (IAA), and with auxin transport inhibitor, *N*-1-naphthylphthalamic acid (NPA). Decapitation removes an auxin source but also removes a sink and therefore increases available sucrose (Kebrom, 2017). All mutants and treatments were compared with intact WT plants. By manipulating the physiological network in this way, we were able to classify different groups of co-expressed genes, providing a solid basis to discover new research directions for understanding the networks involved in SL and auxin regulation.

2 | RESULTS

2.1 | Overview and functional enrichment

Fully elongated hypocotyls were used as the tissue sample in this study of signals regulating SL biosynthesis genes, because grafting experiments have demonstrated that WT hypocotyls can inhibit branching in SL biosynthesis mutant plants (Bainbridge et al., 2005; Beveridge, 2000; Hayward et al., 2009). Gene expression was profiled from the hypocotyls of 2-week-old Arabidopsis WT (1) intact (WT_Intact), (2) decapitated (WT_Decap), (3) decapitated and treated apically with auxin (WT_Decap_IAA) and plants (4) treated with the auxin transport inhibitor NPA (WT_NPA), as well as of mutants in SL biosynthesis and signaling genes: (5) *max1*, (6) *max2*, (7) and *max3*. Cell expansion and growth have ceased in hypocotyls by the treatment time of 2 weeks, making this tissue even more attractive to look at gene regulation caused by genotype and treatment (Gendreau et al., 1997). The mutants and treatments all affect the SL pathway in some way. *max1* and *max3* are deficient in SLs, whereas *max2* cannot perceive SLs. Decapitated and NPA-treated samples inhibit auxin delivery to the hypocotyl, thus affecting SL biosynthesis gene expression (Brewer et al., 2009; Hayward et al., 2009). Decapitation + IAA treatment replaces the loss of auxin in decapitated samples and so helps determine processes that are not solely auxin regulated.

The physiological treatments had a relatively strong effect on the transcriptome. As expected, principal component analysis (PCA) analysis of the normalized intensity values showed clustering of the replicates of each treatment/mutant. The first component (57.07%) discriminated between the plants according to physiological treatments (Figures 1a and S1). The second component (11.7%) separated SL mutants from WT_Intact and WT_Decap_IAA. As might be expected, all SL mutants were clustered together and WT_Decap is close to WT_NPA on the graph, indicating overlapping transcriptional responses (Figures 1a and S1). Results of differentially expressed gene (DEG) analysis relative to the WT_Intact are shown in Figure 1b and Table S1. Genes were deemed "differentially expressed" by absolute LogFC > 2 (|LogFC≥2|) compared with WT expression values and using an adjusted *P*-value (adj *P*-value) cut-off of .05 to assign statistical significance. The highest number of DEGs was observed in the WT_Decap (1097) and WT_NPA (1111) treatments, which indicates dynamic transcriptional responses for these treatments. Applying auxin after decapitation decreased the number of DEGs compared with WT_Decap (292). Many DEGs are shared among the three *max* mutants, and differences between them are discussed below. The combined DEGs of the three *max* mutants (246 combined) were fewer than any of the individual physiological treatments (Figure 1b).

Affymetrix probe IDs of the DEGs were used for functional enrichment of biological processes based on gene ontology (GO) (Ashburner et al., 2000) using the Database for Annotation, Visualization and Integrated Discovery (DAVID) v6.8 (Huang et al., 2009). Functional enrichment analysis showed that many biological processes were differentially regulated among treatments/mutants forming a distinction that mimics the clustering pattern observed by PCA analysis (Figure 1a). There was commonality in the enriched biological processes (GO terms) from DEGs of the three *max* mutants compared with WT (Figure 1c). WT_Decap and WT_NPA also share many common GO terms, apart from the response to auxin group, which was identified for all WT treatments, but not the mutants. The WT_Decap_IAA GO terms were largely unique compared with other WT samples. Some details of these differences are described below together with a co-expression analysis.

2.2 | Co-expression analysis reveals three distinct clusters pertaining to SL biosynthesis and signaling

Gene regulatory networks are used to characterize the correlation patterns among genes. Groups of genes that are correlated in their

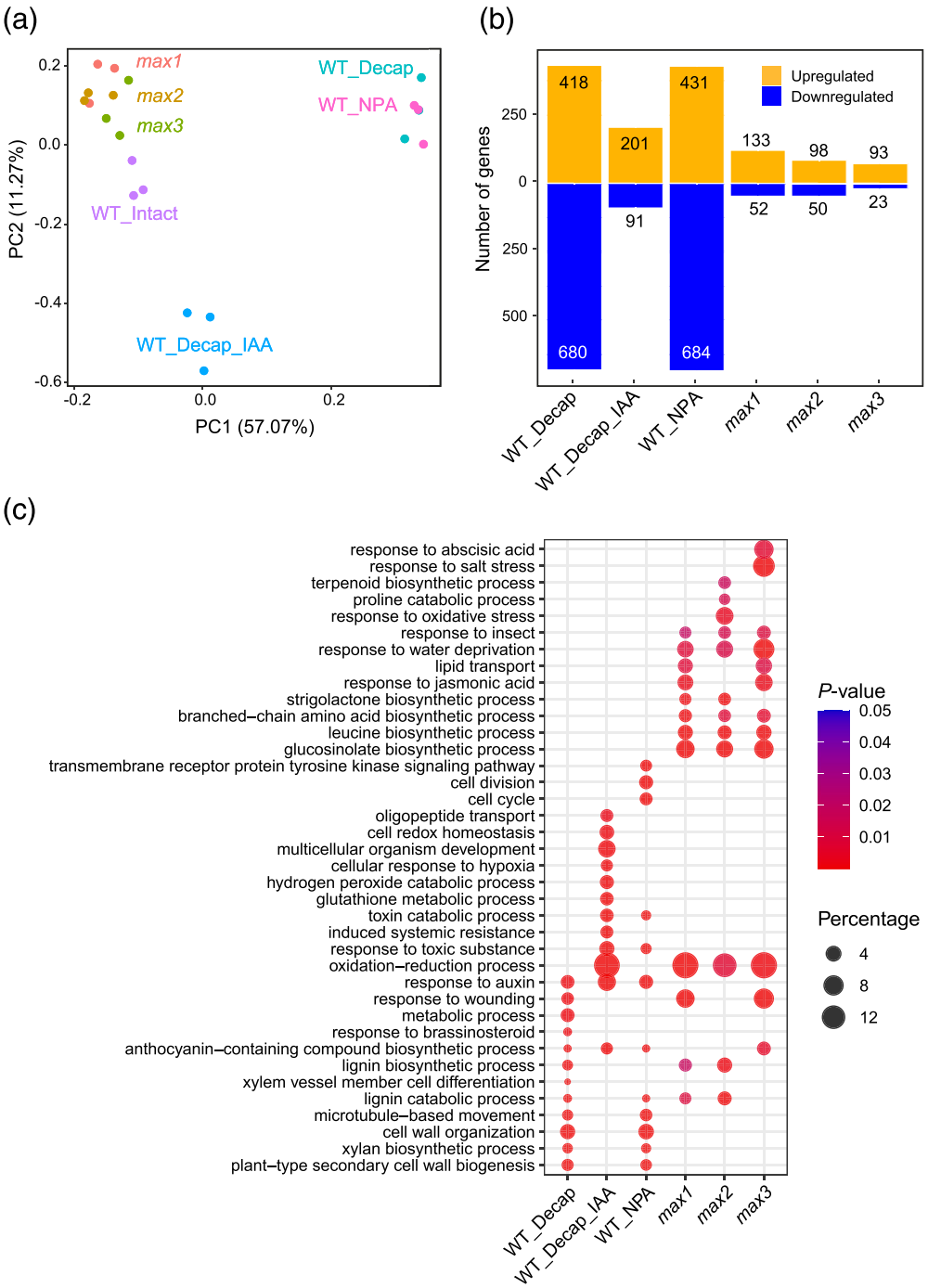

FIGURE 1 Whole-genome differential gene expression analysis. (a) Clusters of samples based on similarity determined by principal component analysis (PCA) show *max* mutants clustering together and close to wild-type intact (WT_Intact) and separate from two other clusters that contain decapitated (WT_Decap) and *N*-1-naphthylphthalamic acid (NPA)-treated (WT_NPA) plants separate from decapitation + indole-3-acetic acid (IAA) (WT_Decap_IAA)-treated plants. (b) Total number of differentially expressed genes (DEGs) when compared with WT_Intact. Genes with a LogFC of two and an adjusted *P*-value of <.05 were considered differentially expressed. WT_Decap- and WT_NPA-treated samples have the largest number of DEGs. The three strigolactone mutants show a much smaller transcriptional response. (c) Gene ontology (GO) categories enriched from DEGs identified in (b). GO terms determined using Database for Annotation, Visualization and Integrated Discovery (DAVID) online database for GO enrichment analysis (Dennis et al., 2003) with a *P*-value of <.05 are considered significantly enriched. Percentage indicates the number of genes differentially expresses in that GO term as a percentage of total genes in that GO term for Arabidopsis.

pattern of expression cluster to form modules that can often be linked to biological functions, such as hormonal biosynthesis. Weighted gene co-expression network analysis (WGCNA) was used to construct gene networks and detect modules of genes (Langfelder & Horvath, 2008). We obtained a network with scale-free topology composed of 26 modules of gene expression correlated with mutants and/or physiological treatments (Figures 2 and S2). WGCNA assigned to each module a unique color label that was used as a specific module identifier in the analyses. The modules were composed, on average, of 437 genes (median gene number per module, 159). The "gray" (or improper) module contains 346 probe sets that were not allocated in any of the 26 modules.

We identified three modules of interest relevant to the SL pathway and which indicated separation of co-expression among genes of the SL pathway. These modules each contained a *MAX* gene described henceforth as module type genes: *MAX3* in brown (617 genes), *MAX1* in blue (1921 genes), and *MAX2* in turquoise (4238 genes) (Figure 2 and Table S2). Genes in the *MAX3* module broadly showed an increase in expression in the SL mutants compared with WT. The *MAX1* and *MAX2* modules differed compared with the *MAX3*, showing a relatively modest change in expression in SL mutants, with a clear response to NPA and to decapitation, which was restored with auxin. The three SL-type genes and their neighbors (strongly correlated genes; $P < .05$) were extracted into

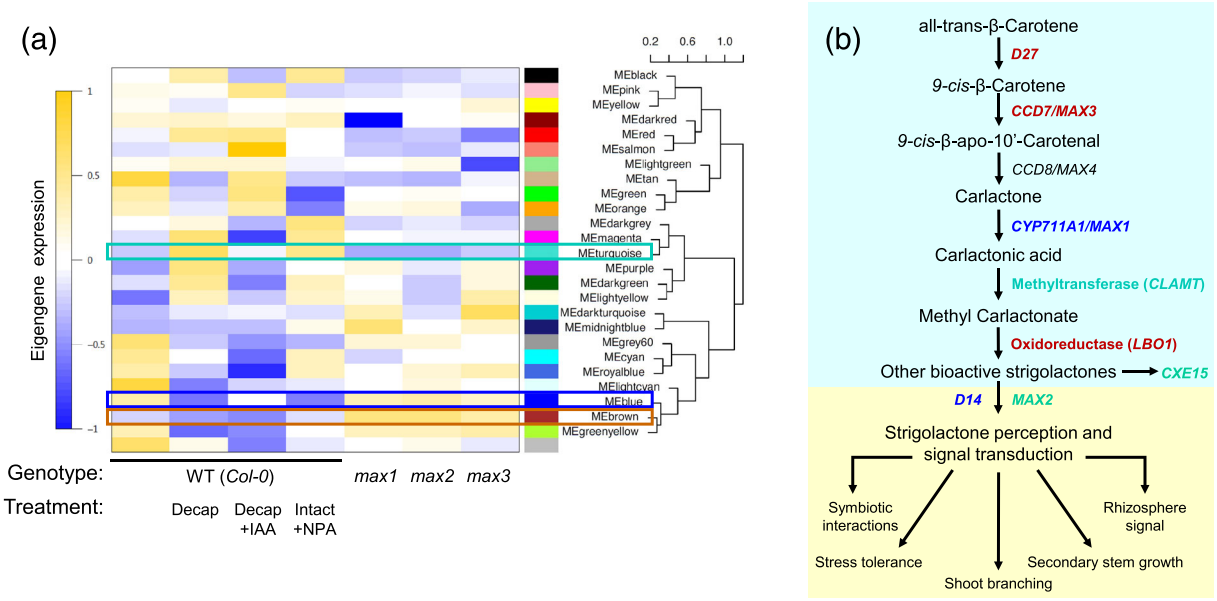

FIGURE 2 Weighted gene co-expression network analysis separates strigolactone (SL) genes into different co-expression groups. (a) Heat map and dendrogram of 26 identified groups of genes based on the pattern of gene co-expression across the entire dataset. Three groups were identified to contain SL genes of interest: *MAX1* (blue), *MAX2* (turquoise), and *MAX3* (brown) (Table S2). (b) Diagram of SL biological pathway. The color of the text of the genes indicates the co-expression group to which they belong.

groups, and the data were used to create a GO term network using the ClueGO extension in cytoscape for each module (Figure S3 and Table S2).

The *MAX3*-like group was extracted from the brown module (224 out of the 617 genes). It consists of SL biosynthesis genes *MAX3*, *MAX4*, *D27*, and *LBO* (Figures 2 and 3) and is also enriched in genes involved in glucosinolate (GSL) biosynthesis pathway (Figure S3) as discussed later. The *MAX3*-like group is categorized by a pattern of differential expression in the *max* mutants.

The *MAX1*-like group was extracted from the blue module (736 out of the 1921 genes) and includes *MAX1* and the SL signaling gene *D14* but also includes genes involved in T6P synthesis, *TREHALOSE 6-PHOSPHATE SYNTHASE 1* (*TPS1*), and dephosphorylation, like *TREHALOSE 6-PHOSPHATE PHOSPHATASE E* (*TPPE*) (Figure 3b). This group is characterized by having genes with differential expression in decapitated and NPA-treated samples. Although *MAX1* and *D14* are upregulated in these samples, *TPS1* and *TPPE* are downregulated; both correlated and anti-correlated genes are included (Figure 3b).

The *MAX2*-like group, which was extracted from the turquoise module (1341 out of the 4238 genes), contains *MAX2* and is enriched in genes involved in auxin and light signaling (Figures 3b and S3). The recently discovered SL catabolism gene *CARBOXYLESTERASE 15* (*CXE15*) and the carlactonic methyltransferase (*CLAMT*) both belong in the turquoise co-expression module with *MAX2* (Mashiguchi et al., 2022; Wakabayashi et al., 2021; Xu et al., 2021) (Figure 3b and Table S2). However, neither genes were strictly co-expressed with *MAX2* and so are not included in the *MAX2*-like group.

2.3 | Treatments with WT plants highlight auxin-responsive genes and anthocyanin pathway genes

As expected, DEGs in common from WT_Decap, WT_Decap_IAA, and WT_NPA plants are enriched in the auxin-activated signaling pathway category (Figures 1a and 4a). Genes involved in anthocyanin-containing compound biosynthesis were enriched in WT_Decap, WT_Decap_IAA, and WT_NPA plants (Figures 1c and 4). Anthocyanin biosynthesis genes such as *UDP-GLUCOSE:FLAVONOID 3-O-GLUCOSYLTRANSFERASE* (*UF3GT*), *MYB75/PRODUCTION OF ANTHOCYANIN PIGMENT 1* (*PAP1*), and *DIHYDROFLAVONOL 4-REDUCTASE* (*DFR*) are largely repressed in these treated WT plants compared with untreated WT (Figure 4b). Among the genes that showed common expression among all the treated WT plants (decapitation with or without IAA and intact with NPA), compared with intact WT, were 75 genes also differentially expressed between WT and SL mutants. Some of these were in the anthocyanin group although not suppressed in the mutants to the extent in WT treated plants (Figure 4b). Previous studies have shown effects of sugars and auxin on anthocyanin content (Ozeki & Komamine, 1986; Teng et al., 2005). Additionally, MAX2 was suggested to impact anthocyanin content, as *max2* mutants have downregulated anthocyanin biosynthesis gene expression (Richmond et al., 2022). This potential regulation of anthocyanins has not been widely repeated and is yet to be tested by direct measurement of anthocyanin levels, or related to the high endogenous auxin or auxin signaling in SL mutants. Therefore, we measured anthocyanin content in whole rosettes of WT (Col-0), *max2*,

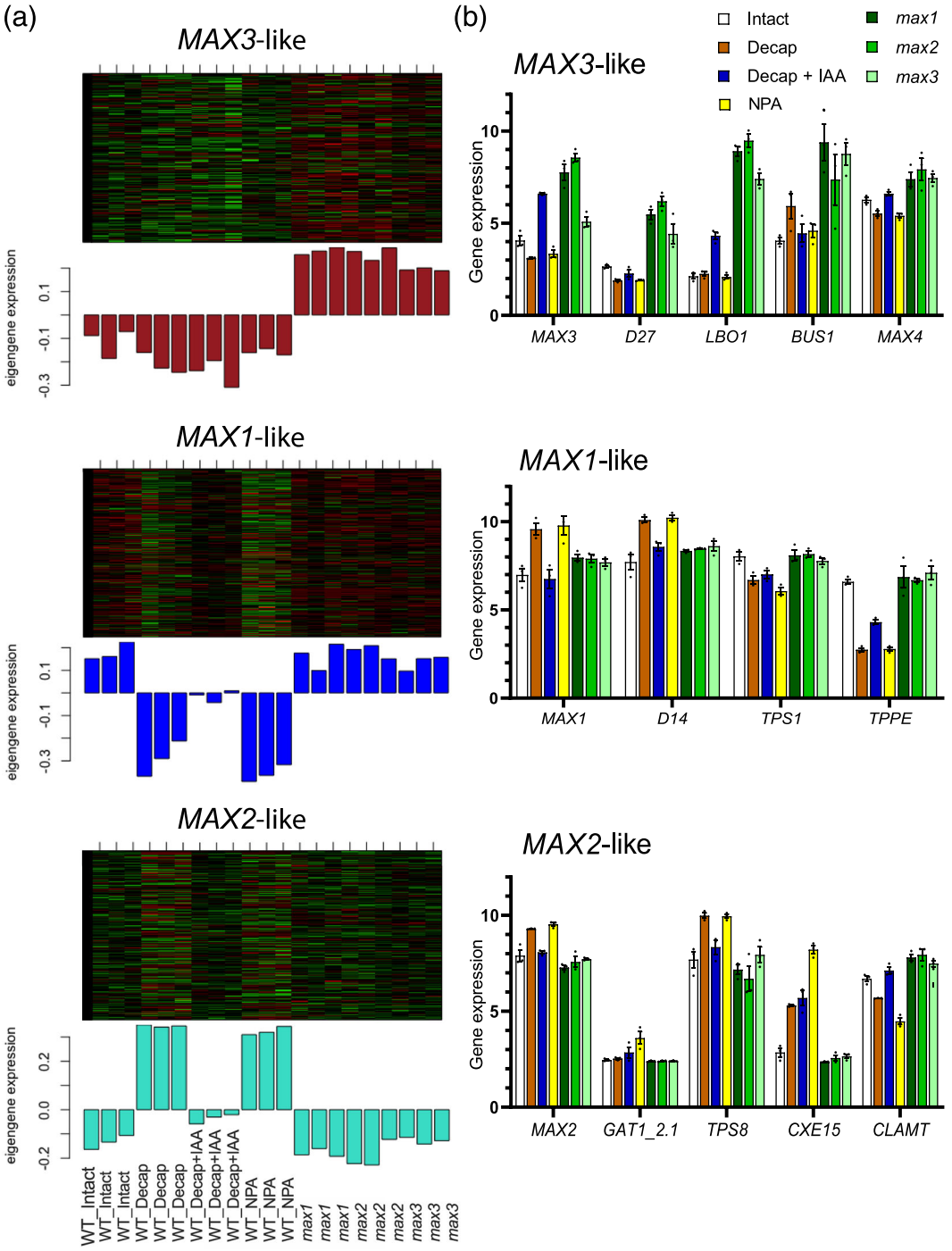

FIGURE 3 Functional analysis of strigolactone (SL)-like co-expression groups. (a) Eigengene expression in individual replicates for *MAX3*-like, *MAX1*-like, and *MAX2*-like co-expression groups identified in Figure 2. (b) Absolute gene expression as raw robust multichip average values of representative genes from each MAX-like co-expression group. Data presented as mean ± SEM ($n = 3$).

d14, and in the auxin-overproducing line *35S:YUCCA1* (Zhao et al., 2001). High auxin content plants, *35S:YUCCA1*, did in fact have the highest accumulation of anthocyanins, and *max2* had significantly lower anthocyanin accumulation than both WT and *35S:YUCCA1* plants (Figure 4c).

2.4 | SLs may be strongly associated with GSLs in Arabidopsis

We sought to identify and characterize DEGs common among the *max* mutants used in this study. Thirty-seven genes were common

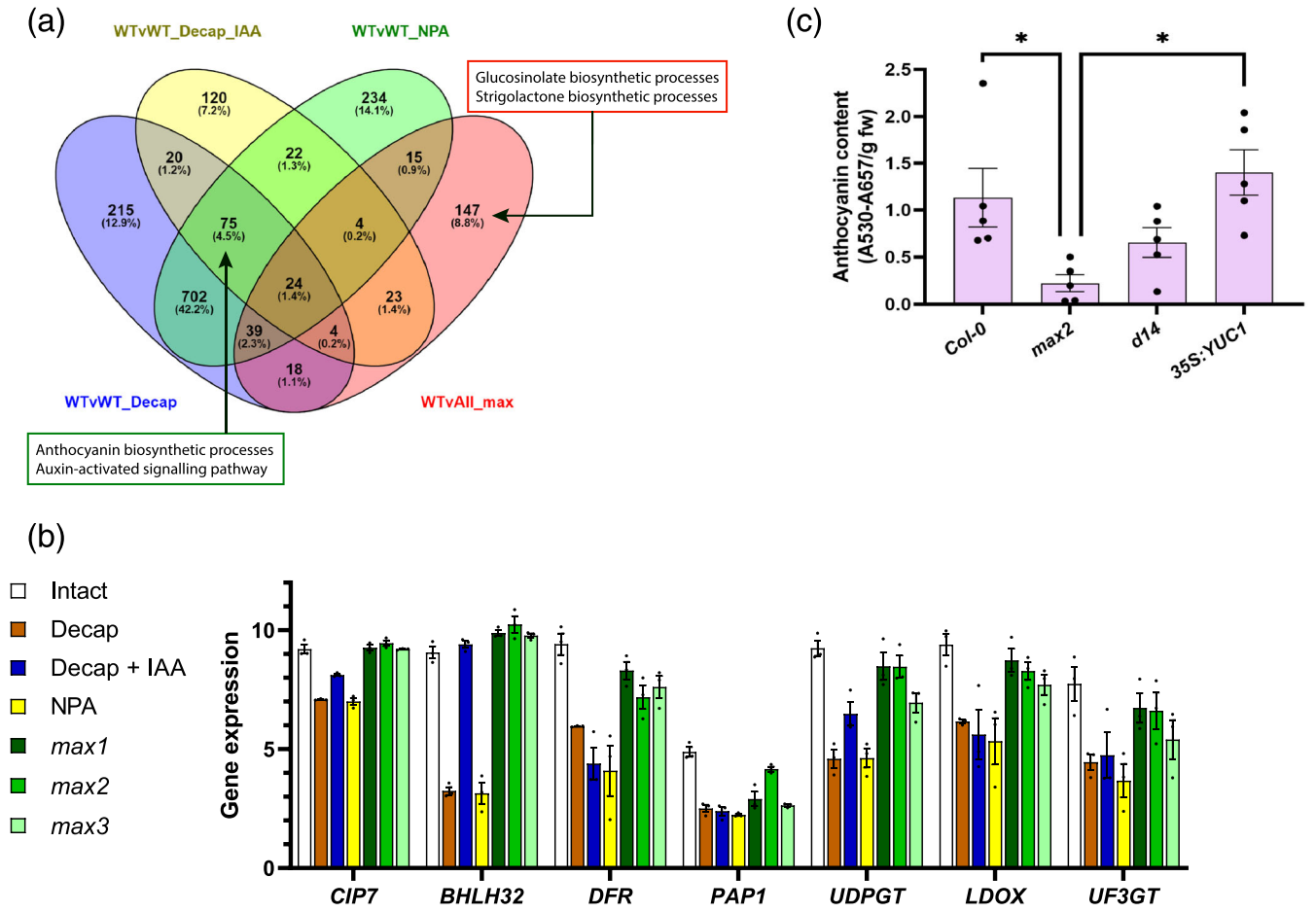

FIGURE 4 Hormonal perturbations regulate anthocyanin biosynthesis and accumulation. (a) Overlap of differentially expressed genes (DEGs) for the entire data set. *Max* mutant DEGs are combined to represent the entire strigolactone (SL) mutant transcriptional response. Percentages in each bubble represent the percentage of all genes in the entire Venn diagram in that bubble. Top two gene ontology (GO) terms for *max*-specific (differentially expressed in only *max* mutants) and treatment-specific (DEGs in common with all three treatments, but distinct from *max* mutants) are highlighted. *Max* mutants independently display changes in glucosinolate biosynthesis and SL biosynthesis. Physiological treatments affect anthocyanin biosynthesis and auxin signaling. (b) Absolute gene expression as raw robust multichip average values for differentially expressed anthocyanin biosynthesis genes identified in 4A. (c) Anthocyanin measurements in whole rosettes of WT (Col-0), *max2*, *d14*, and *35S:YUCCA1* at 4 weeks old. Data presented as absorbance at 530 nm−absorbance at 657 nm per gram of fresh weight. Mean ± SEM ($n = 5$) unpaired two-tailed Students *t*-test *P*-value of <.05.

DEGs among all *max* mutants (Figure 5a). These genes are significantly enriched for GSL biosynthetic processes (*P*-value: $7.50e^{-6}$) (Figures 5b and S4 and Table S3). Further investigation determined that all these GSL genes belonged to the process of, specifically, aliphatic GSL (aGSL) biosynthesis. Some aGSLs are derived from branched chain amino acids, and the biosynthesis of these branched chain amino acids was also a significantly enriched GO term for all the *max* mutants (Figure 1c). Over 40% of all aGSL biosynthesis genes are upregulated in the SL mutants (Figures 5c and S4). For example, GSL biosynthesis genes *MYB29*, *CYTOCHROME P450 79F1/BUSHY 1* (*CYP79F1/BUS1*) (henceforth referred to as *BUS1*), *ISOPROPYLMALATE ISOMERASE 1* and *2* (*IPMI1* and *IPMI2*), and *BILE ACID TRANSPORTER 5* (*BAT5*) are upregulated in all three *max* mutants (Figure 5b) and appear to be highly expressed specifically in the leaf axils of plants (Figure S5) (Tantikanjana et al., 2001; Winter et al., 2007). Interestingly, the *bus1* mutant has a bushy growth phenotype (Hansen et al., 2001; Reintanz et al., 2001; Tantikanjana et al., 2001). SL analog, GR24, can be used to complement the hyperbranching phenotype of the SL deficient biosynthesis mutants *max1*, *max3*, and *max4* but not in SL signaling mutants, for example, *max2* (Gomez-Roldan et al., 2008; Umehara et al., 2008). To determine whether *BUS1* is involved in SL biosynthesis, GR24 was applied to rosette buds of WT (Col-0), *max4*, *max2*, and *bus1* mutants. Consistent with published results, GR24 complements the branching phenotype of the *max4* mutant but not the *max2* mutant (Figure 5d). Similarly, the enhanced branching phenotype of *bus1* cannot be complemented by GR24 application suggesting that GSL's connection to branching inhibition might be downstream of SL signaling (Figure 5d).

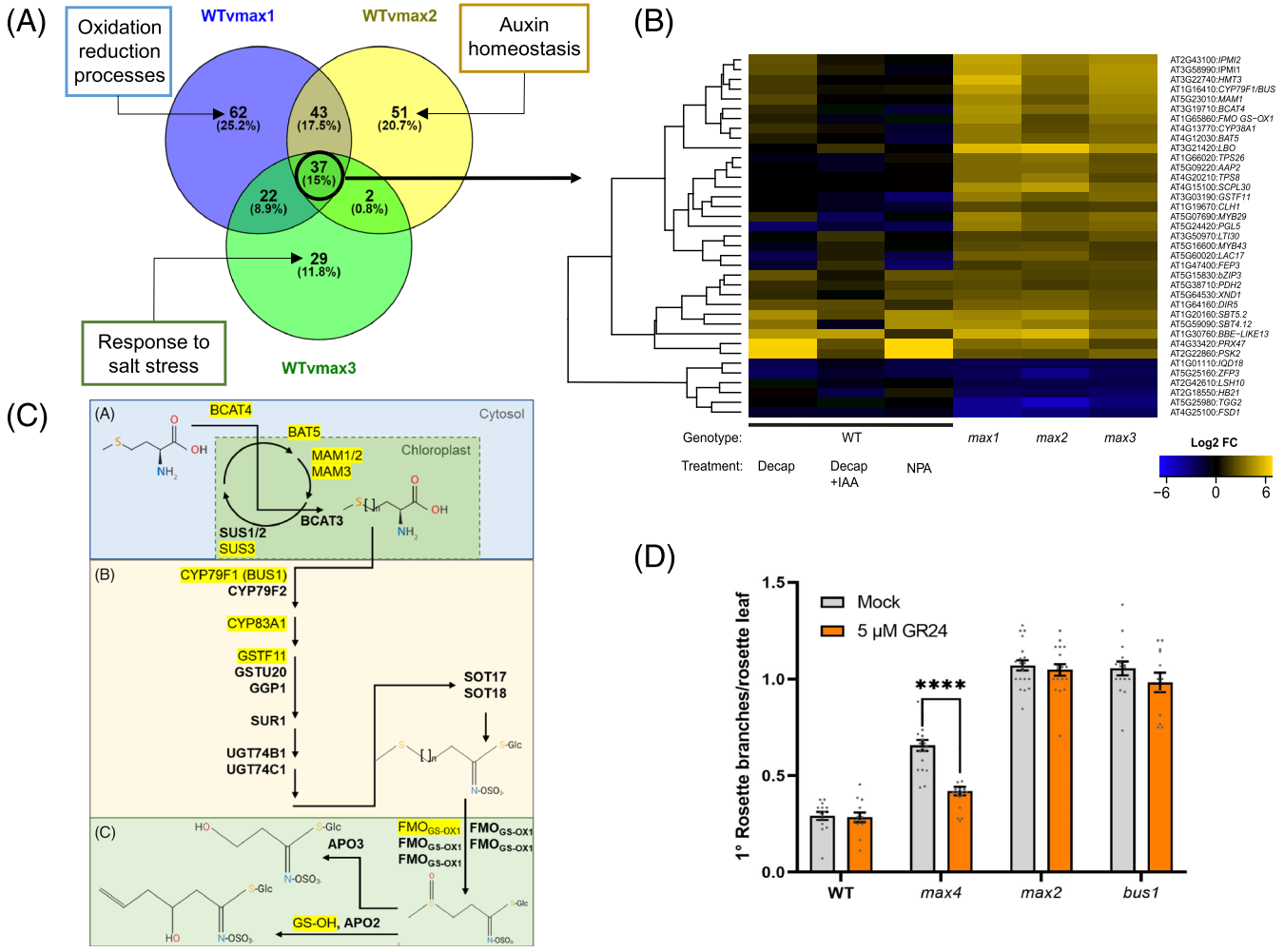

FIGURE 5 Strigolactone (SL) mutants highly upregulate glucosinolate biosynthesis. (a) Overlap between differentially expressed genes (DEGs) for *max1*, *max2*, and *max3* mutants. Top gene ontology (GO) term for each individual mutant is highlighted (full list in Table S3). Percentages in each bubble represent the percentage of all genes in the entire Venn diagram in that bubble. (b) Expression for the 37 genes commonly identified as differentially expressed in max mutants. This gene list shows enrichment in glucosinolate metabolism. (c) Diagram of aliphatic glucosinolate biosynthesis pathway showing genes (highlighted in yellow) that are upregulated in max mutants. The aliphatic glucosinolate biosynthesis pathway is split into three components: (A) chain elongation, part of which occurs in the chloroplast; (B) biosynthesis of core glucosinolate structure; and (C) secondary modifications. For more detailed explanation, see Sønderby et al., 2010). (d) Exogenous SL (GR24) does not restore high branching phenotype of the *bus1* mutant to WT. Data are presented as mean ± SEM ($n = 13–20$) two-way ANOVA *P*-value of <.0001.

2.5 | SL negative feedback is only partly regulated by auxin

Consistent with previous reports, we find that SL biosynthesis genes *D27*, *MAX4*, *MAX3*, and *LBO* are upregulated in *max1*, *max2*, and *max3* SL mutant hypocotyls (Bennett et al., 2006; Brewer et al., 2016; Hayward et al., 2009; Shen et al., 2012; Waters, Brewer, et al., 2012) (Figure 6a). This negative feedback loop has been suggested to be auxin mediated (Hayward et al., 2009; Ligerot et al., 2017). However, if auxin was solely responsible, exogenous auxin would be expected to result in the same increase in SL biosynthesis gene expression as observed in SL biosynthesis mutants. Using a transcriptomic approach, we can confirm auxin uptake and signaling by examining transcriptional responses of auxin-related genes. Here, we used a ratio of the fold change gene expression compared with WT_Intact across all three *max* mutants used in this study to the fold change gene expression in WT_Decap_IAA compared with WT_intact plants (Figure 6b). A ratio of 1 (the *x*-axis) would indicate that IAA/auxin application to decapitated plants has the same effect on SL biosynthesis as an SL biosynthesis gene mutation, a ratio below 1 indicates high auxin regulation (bars below the *x*-axis), and a ratio above 1 indicates that it is something different in the SL mutants causing gene expression changes (bars above the *x*-axis) (Figure 6b). Genes covering the major classes of auxin-responsive genes (*PIN*, *IAA*, *GH3*, and *SAUR*) were selected to compare against. For all 16 auxin-responsive genes, the ratio of gene expression is equal to or less than one, implying that their expression can mostly be explained by the

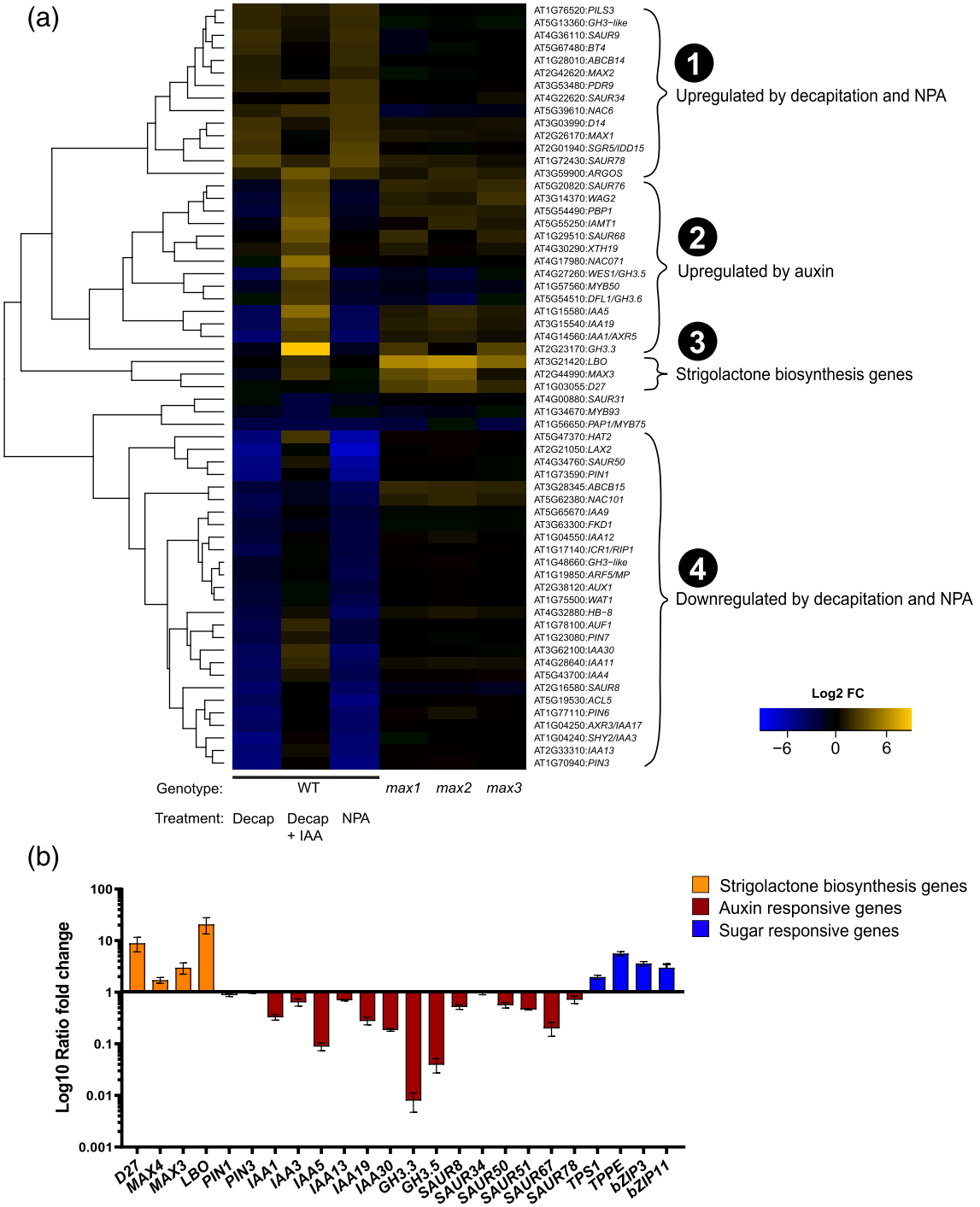

FIGURE 6 Feedback regulation of strigolactone (SL) biosynthesis genes in SL mutants is predominantly auxin-independent. (a) Auxin-related genes in SL mutant hypocotyls show similar expression to WT. Significant ($P = .1$) auxin-related genes were derived from gene ontology (GO) terms from differentially expressed genes (DEGs) from WT_Decap_IAA and WT_NPA treatments. Cluster 1 contains auxin-related genes upregulated in WT_Decap and WT_NPA consistent with inhibition of polar auxin transport. Cluster 2 contains genes typically upregulated by auxin. Cluster 3 contains SL biosynthesis genes (except *MAX1*). Cluster 4 contains genes downregulated by WT_Decap and WT_NPA treatments. (b) The ratio of fold change in *MAX* mutants and fold change in WT_Decap_IAA treated show selected SL biosynthesis (in orange), and sugar responsive genes (in blue) are highly expressed in SL biosynthesis mutants compared with auxin-treated samples. Auxin-responsive genes (in red) all show a low (≤1) ratio of *MAX*: WT_Decap_IAA fold change expression indicating predominantly auxin regulation of expression.

addition of auxin (red bars in Figure 6b). However, the ratio of gene expression for SL biosynthesis genes *D27*, *MAX4*, *MAX3*, and *LBO* are all above 1 (orange bars in Figure 6b). A high ratio indicates that auxin alone is not responsible for the increased SL biosynthesis and provides circumstantial evidence for non-auxin feedback on SL biosynthesis gene expression.

Several sugar-responsive genes were highlighted as being co-regulated with the SL biosynthesis gene, *MAX1* (Figure 3b). When the fold change gene expression ratio between SL mutant and IAA-treated plants is applied to these genes, they also show a ratio above 1, like the SL biosynthesis genes (blue bars in Figure 6b). This indicates that these sugar-responsive genes are also not solely controlled by auxin. Using available data from several microarray experiments through Genevestigator (Hruz et al., 2008), we confirmed that SL genes are more responsive to treatments with sugar perturbations than those with auxin perturbations (Figure S6). *MAX1* is not included in this analysis because unlike other SL biosynthesis genes (*D27*, *MAX4*, *MAX3*, and *LBO*), *MAX1* is not upregulated in any SL mutant. However, *MAX1* is upregulated by decapitation and NPA treatments. (Figure 6a). The SL receptor genes *MAX2* and *D14* are both also upregulated in WT_Decap and WT_NPA (Figure 6a). This indicates that transcriptional regulation of *MAX1* in response to auxin is more similar to *MAX2* and *D14* than to *D27*, *MAX4*, *MAX3*, and *LBO*.

3 | DISCUSSION

In this study, we used whole genome differential gene expression and WGCNA to study transcriptional changes and patterns associated with disruptions to the SL pathway in Arabidopsis to identify potential new interactions between SL and other pathways. WT_Decap and WT_NPA treatments showed the largest transcriptional responses and were quite similar (Figure 1a). This is consistent with the shoot tip being a source of auxin and affecting multiple aspects of development. WT_Decap_IAA showed fewer DEGs than WT_Decap alone, consistent with auxin being able to restore some, but not all of the transcriptional response caused by decapitation (Cline, 1996; Crawford et al., 2010). This comparison of the treatments in WT enables a grouping of genes involved in the auxin-independent decapitation responses including wounding and loss of the main shoot sink tissue, the shoot tip. In contrast, relative to these large responses, mutants in SL signaling have comparatively few transcriptional differences compared with WT_Intact. It is often noted that very few genes are transcriptionally regulated by the loss of SLs compared with other plant hormones (Lantzouni et al., 2017; Mashiguchi et al., 2009; Smith & Li, 2014; Wang et al., 2020), which is somewhat surprising given the number of phenotypic differences in SL mutants compared with WT plants (Brewer et al., 2013).

Differential gene expression across this study has highlighted enrichment of genes involved in secondary metabolite biosynthesis, particularly anthocyanins and GSLs, indicating that plant defense mechanisms are being modulated by SL and physiological perturbations in Arabidopsis. Transcriptional responses unique to and common to all of the *max* mutants included altered expression of GSL biosynthesis genes, and it is therefore likely that a connection exists between SLs and GSLs (Figure 5). Previous research showed that Arabidopsis mutants deficient in key steps of the GSL biosynthesis had increased shoot branching, indicating a potential role for GSLs in the regulation of shoot architecture besides their key role in defense (Bak & Feyereisen, 2001; Hansen et al., 2001; Reintanz et al., 2001). Anthocyanin biosynthesis genes are downregulated across the data set, particularly by physiological treatments (Figure 4b). It is likely that SL and auxin are together enhancing anthocyanin biosynthesis (Ha et al., 2014; Patil et al., 2021). Additionally, we revealed some evidence for non-auxin-mediated negative feedback on SL biosynthesis.

3.1 | Interaction between SLs and GSL metabolism

GSLs are secondary metabolites characteristic of the *Brassicaceae* family. GSLs can be divided into three groups based on their amino acid precursor. aGSLs are derived from Ala, Leu, Ile, Val, and Met (Figure 5c uses methionine as an example), benzenic GSLs are derived from Phe or Tyr; and indolic GSLs are derived from Trp (Sønderby et al., 2010). The major role for GSLs in plants lies in their toxicity to insects, thus preventing herbivory (Chew, 1988; Halkier & Gershenzon, 2006). However, with over 100 known GSLs with more than 40 different genes involved in GSL biosynthesis, it is likely that GSLs perform a wide range of roles in plants (Francisco et al., 2016; Sønderby et al., 2010). Indeed, a number of GSL mutants exhibit significant growth defects, including enhanced shoot branching and adventitious rooting; thus, it is likely that cross-talk between plant hormones and GSL biosynthesis occurs (Burow et al., 2015; Burow & Halkier, 2017; Francisco et al., 2016; Robert-Seilaniantz et al., 2011).

All three of the SL mutants showed significant upregulation of genes in the aGSL biosynthesis pathways, indicating that SLs might be inhibiting GSLs (Figures 4, 5c, and S4) (Sønderby et al., 2010). Of genes commonly upregulated by *max* mutants (Figures 5B and S4), the transcription factor *MYB29* regulates the expression of aGSL biosynthesis genes in Arabidopsis, including *BAT5*, which belongs to the bile acid transporter family (Araki et al., 2013; Zhang et al., 2017; Zuluaga et al., 2019). *IPMI1* and *IPMI2*, which catalyze plastidic chain elongation reactions, are also targets of *MYB29* (Augustine & Bisht, 2017; Gigolashvili et al., 2009; Sønderby et al., 2010). *BUS1* and *CYP79F2* perform partially redundant functions in aGSL synthesis in Arabidopsis (Chen et al., 2003; Hansen et al., 2001). *bus1* single and *bus1/cyp79f2* double-knockout plants are GSL deficient (Reintanz et al., 2001; Tantikanjana et al., 2004). Interestingly, like *max* mutants, *bus1* Arabidopsis mutants exhibit an increased branching phenotype (Reintanz et al., 2001) (Figure 5d). Given that exogenous SL is unable to recover the mutant *bus1* phenotype, it is possible that aGSLs are regulated downstream of *MAX2* (Figure 5d). *bus1* plants are aGSL deficient; however, the *max* mutants (also showing a bushy phenotype) show enhanced aGSL biosynthesis further suggesting that aGSL inhibition of shoot branching is not due to inhibiting SL biosynthesis and may be activated as part of a feedback process to suppress branching under SL deficiency. It is likely that SLs and GSLs are working together to some extent as shoots of *bus1* and SL mutants have higher levels of endogenous cytokinins (Tantikanjana et al., 2001; Young et al., 2014). The increase in CK levels in *bus1* is far higher than

ever reported for SL mutants and this is consistent with the observation that CK pathways were upregulated in WT_Decap and WT_NPA but not in SL mutant hypocotyls (Table S3).

Auxin signaling has been found to affect aGSL levels in Arabidopsis. Triple-knockout *iaa5/iaa6/iaa19* plants have reduced aGSL levels and impaired drought tolerance. Application of GSLs to these mutants restores the stomatal regulation and drought tolerance (Salehin et al., 2019). *IAA5*, *IAA6*, and *IAA19* are well-known auxin-responsive genes (Weijers & Wagner, 2016) and were strongly promoted by auxin (Figure 6a). *IAA5* and *IAA19* expression was decreased in WT_Decap and WT_NPA treatments and increased in WT_Decap_IAA compared with WT (Figure 6a). These treatments had, comparatively, little or no effect on aGSL biosynthesis transcript levels (Figure S4C,D) compared with the high level of promotion in SL mutants. This indicates that high level of aGSL gene expression in SL mutants is not simply due to auxin signaling.

HOMEOBOX PROTEIN 21 (*HB21*) is among the 37 common DEGs between the three SL mutants (Figure 5b) and is downregulated in the *max* mutants. *HB21* is a direct target of *BRANCHED1* (*BRC1*), the central integrator of shoot branching signals (Wang et al., 2020), and acts redundantly with HB40 and HB53 to inhibit branching (González-Grandío et al., 2017; Whipple et al., 2011). *BRC1* is downregulated in axillary buds of SL mutants (Braun et al., 2012; Dun et al., 2012). Because of *BRC1* unfortunately not being a probe on the Affymetrix chip, we could not test *BRC1* expression directly. However, as *BRC1* is a well-established, bud-specific marker gene, we do not anticipate *BRC1* expression in the hypocotyl (Figure S8) (Aguilar-Martínez et al., 2007; Braun et al., 2012; Klepikova et al., 2016). Therefore, *HB21* downregulation in hypocotyls of *max* mutants might be independent of BRC1. Interestingly, *HB21* is also known to regulate GSL accumulation, and *hb21* mutant Arabidopsis plants have diminished aGSL levels (Li et al., 2014, 2018), further linking SL signaling, aGSL biosynthesis, and branching in Arabidopsis.

Another established aspect of SL signaling is the promotion of associations with AM fungi (Bouwmeester et al., 2007). However, many *Brassica* species do not form associations with AM fungi, including Arabidopsis (Kruckelmann, 1975). GSLs are a characteristic of brassicas and so may be part of the explanation that these plants cannot form symbiotic associations. GSLs have been linked to impacting microbe diversity in the rhizosphere (Bressan et al., 2009; Burow & Halkier, 2017). Additionally, Arabidopsis GSL biosynthesis genes are upregulated in response to AM fungi colonization in a neighboring host (Fernández et al., 2019). It may be that GSL biosynthesis is upregulated in this situation to inhibit AM fungi colonization although the spores are present. The SL involvement in AM fungi associations is likely a conserved response (Fernández et al., 2019; Lanfranco et al., 2018), but perhaps SLs can somewhat inhibit the GSL-mediated inhibition of AM fungi (Figure 7). GSL measurements in SL mutants in Arabidopsis as well as monitoring AM fungi colonization in non-GSL-producing Arabidopsis mutants and regular AM host species in response to different SL and GSL treatments would be needed to better understand this interaction.

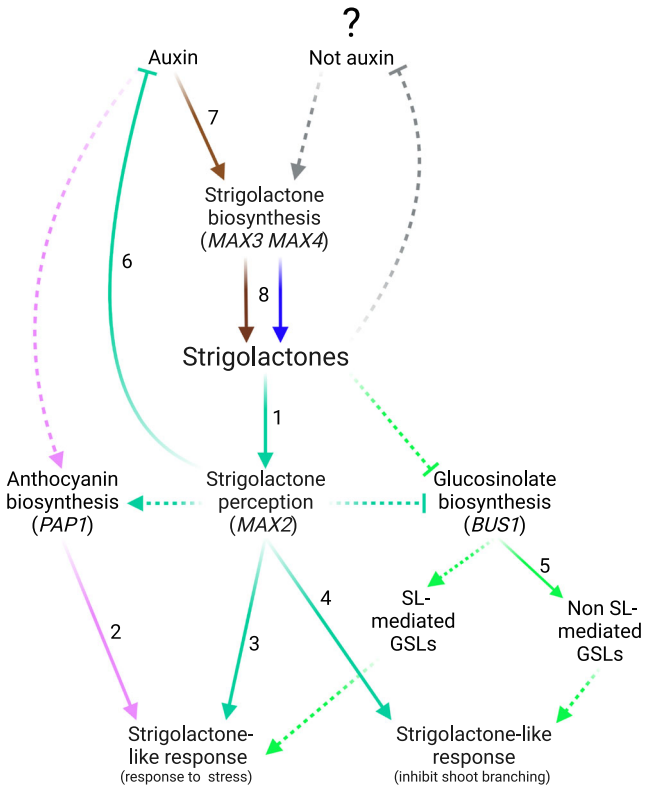

FIGURE 7 Summary of strigolactone (SL) signaling. Model of SL regulation of secondary metabolites and non-auxin-mediated feedback on SL biosynthesis. Dashed lines indicate ideas reported in this manuscript. Numbers are references to previously published interactions. (1) Hamiaux et al. (2012). (2) Landi et al. (2015). (3) Pandey et al. (2016). (4) Stirnberg et al. (2002). (5) Sønderby et al. (2010). (6) Ligerot et al. (2017). (7) Hayward et al. (2009). (8) Gomez-Roldan et al. (2008).

3.2 | Interactions between SLs and anthocyanins

Anthocyanins are an important class of flavonoids that represent a large group of ubiquitous plant secondary metabolites (Liu et al., 2018). They are glycosylated polyphenolic compounds involved in stress responses, especially high light and nutrient stress and so are fundamental in plants and their adaptation to the environment (Liu et al., 2018; Tanaka et al., 2008). Anthocyanins also largely play a protective role in plants (Agati et al., 2012; Gould et al., 2002; Landi et al., 2015; Zheng et al., 2020). Anthocyanin biosynthesis genes are downregulated compared with WT_Intact, across the data set, but especially in the WT_Decap, WT_Decap_IAA, and WT_NPA plants (Figure 4b). Auxin has been shown to regulate anthocyanin biosynthesis synergistically with cytokinins (Ji et al., 2015; Liu et al., 2014). Cytokinins promote anthocyanin biosynthesis and have been shown to induce *DFR* and *UF3GT* expression (Deikman & Hammer, 1995; Wang et al., 2019). Although co-treatment of auxin and cytokinins significantly enhances cytokinin-induced anthocyanin production, high auxin concentration (>9-μM NAA) strongly inhibits anthocyanin biosynthesis, even in the presence of cytokinin (Ji et al., 2015; Liu

et al., 2014). As well as hormones, sucrose induces anthocyanin production. Sucrose upregulates *PAP1* and *DFR*, which catalyze the first committed step in anthocyanin biosynthesis (Das et al., 2012; Teng et al., 2005). It is possible that altered auxin, cytokinins, or sugar levels in the stem after decapitation enhance anthocyanin biosynthesis.

SLs have also been shown to regulate anthocyanin accumulation in plants (Ferrero et al., 2018; Ito et al., 2015). This could suggest that SLs regulate anthocyanin accumulation downstream of auxin or sugar signaling, supported by *max2* rosettes having decreased anthocyanin accumulation, as *MAX2* is implicated in both auxin and sugar signaling pathways (Figure 4c) (Barbier, Péron, et al., 2015; Ha et al., 2014; Ligerot et al., 2017; Patil et al., 2021). Recent findings have revealed that SLs play a role in anthocyanin accumulation through upregulation of anthocyanin biosynthesis genes such as *PAP1* (Wang et al., 2020). Wang et al. (2020) described *max3* mutants as showing decreased anthocyanin content compared with WT, which our study consolidates, as the *max3* mutant shows decreased expression of anthocyanin biosynthesis genes, including *PAP1* (Figures 4b and 7). MAX2, although being essential to SL reception, is also essential for karrikin signaling by interacting with α/β hydrolase KARRIKIN INSENSITIVE 2 (KAI2) instead of D14 (Nelson et al., 2011; Waters, Nelson, et al., 2012). Karrikins can enhance anthocyanin accumulation, and this accumulation is dependent of KAI2. However, unlike *max2* mutants, *kai2* mutants do not show reduced anthocyanin accumulation compared with WT plants (Bursch et al., 2021). These findings agree with recent suggestions that MAX2 is a master regulator of flavonoid biosynthesis with *max2* showing downregulated flavonoid biosynthesis and metabolism in roots, which is not seen in *max4* or *d14* mutants (Richmond et al., 2022) (Figure 4c).

3.3 | Transcriptional differences among SL biosynthesis mutants

The physiological treatments provide a good framework to identify genes that respond to major signaling changes within the plant relating to shoot branching and apical dominance. SL mutants enable us to narrow down which parts of the framework are specifically involved in regulation of or by SLs.

DEG and WGCNA analyses highlighted differences among SL mutants (Figure 5a). Although an independent function of MAX2 is expected considering its role in the perception (as opposed to biosynthesis) of SL, and its involvement in karrikin signaling, MAX3 and MAX1 act linearly in the SL biosynthesis pathway (Abe et al., 2014; Alder et al., 2012; Nelson et al., 2011; Stirnberg et al., 2007). *MAX1* encodes a cytochrome P450 enzyme that converts carlactone to carlactonic acid, whereas *MAX3* encodes a carotenoid cleavage dioxygenase that converts 9-*cis*-β-carotene to 9-*cis*-β-apo-10′-carotenal (Figure 2b). Consequently, the *max1* mutant accumulates carlactone, whereas *max3* mutants do not and instead accumulate 9-*cis*-β-carotene. *max1* mutants showed a greater number of transcriptional changes than *max2* and *max3* mutants (Figure 1b). In accordance, another recent microarray analysis of SL mutants also reported a difference in transcriptional responses in the SL mutants, highlighting substantial transcriptional changes in Arabidopsis *max1* mutant leaves compared with other SL mutants (Kumar et al., 2019). A higher transcriptional response in *max1* compared with *max3* might suggest that the build-up of carlactone is biologically relevant. Carlactone added to *max* mutants can inhibit rosette branching in Arabidopsis, even partially in the *max2* mutant background, which is deficient in SL sensing (Abe et al., 2014). Therefore, part of the carlactone effect on shoot branching seems to be not mediated by D14-MAX2 degradation of SMXLs opening a new avenue of enquiry (Abe et al., 2014; Kumar et al., 2019).

3.4 | Feedback regulation of SL biosynthesis

SL mutants have increased expression of SL biosynthesis genes (*D27*, *MAX3*, *MAX4*, and *LBO*), indicative of a negative feedback loop (Figure 6a) (Hayward et al., 2009). The perception of SL by *MAX2* may contribute to negative feedback on SL biosynthesis genes via inhibiting auxin transport (Ligerot et al., 2017). However, auxin may not be solely responsible for negative feedback on SL biosynthesis in SL mutants. Application of auxin neither rescues the enhanced branching phenotype nor SL biosynthesis gene expression back to WT levels in SL mutants, nor does it restore depleted SL contents to roots of decapitated plants (Bennett et al., 2006; Hayward et al., 2009; Yoneyama et al., 2015) (Figures 6a and 7). To further examine the extent of non-auxin feedback regulation of SL biosynthesis gene expression, we plotted the ratio of gene expression in SL mutants to that of the same genes in auxin-treated plants (Figure 6b). If auxin was solely responsible for controlling SL biosynthesis, a ratio of 1, or below, is expected because the high gene expression change in SL mutants would be balanced with the high gene expression of auxin response after auxin treatment. As expected, all auxin-responsive genes (in red; Figure 6b) fall below the threshold of 1. In contrast, all SL biosynthesis genes (in orange) show a very high ratio above 1. The inability of auxin to restore SL biosynthesis gene levels to intact WT levels in *max* mutants suggests some non-auxin-related negative feedback on SL biosynthesis genes (Figure 6b).

Sugars or sugar signaling is a candidate for a non-auxin signal regulating SL biosynthesis gene expression and needs to be tested experimentally. Consistent with this, sugar perturbations generally have a larger effect on the transcriptional regulation of SL biosynthesis genes *MAX1* and *D27* than do auxin perturbations, but this is not the case for *MAX3* (Figures S6 and S7). Given that *MAX3* is not differentially expressed in treatments that affect sugar levels, sugar itself is not a great candidate for a common non-auxin signal regulating SL biosynthesis gene expression.

Sucrose is known to have an inhibitory effect on SL perception (Bertheloot et al., 2020; Fichtner et al., 2021; Patil et al., 2021). Sugar signaling-related genes were strongly correlated with SL genes *MAX1* (i.e., *TPS1* and *TPPE*) and *MAX2* (i.e., *TPS8*) (Figure 3b) raising the hypothesis that sugar signaling could be affecting expression of these genes. *MAX2* expression is suppressed by sugars (Patil et al., 2021),

whereas *MAX1* expression is enhanced (Figure S7). It is important to notice here that regulation of *MAX1* gene expression is different from the other SL biosynthesis genes. In particular, *MAX1* is not as highly expressed in SL mutants than other SL biosynthesis genes (Figure 3b). These similarities in expression among *MAX1*, *MAX2*, and also *D14* suggest that *MAX1* may be regulated by sugars similar to the SL signaling genes (Barbier, Péron, et al., 2015; Bertheloot et al., 2020; Patil et al., 2021). The interactions between auxin, sugars, and SL levels and signaling is therefore an interesting topic for further research.

3.5 | Conclusion

The aim of this research was to identify novel components in the SL regulatory network and to provide a tool for additional network analysis for the regulation of the SL pathway. GSLs and anthocyanins are both highlighted as potentially new targets of SL signaling. Additionally, we present evidence for non-auxin-mediated feedback on SL biosynthesis and propose that components of sugar signaling could be partially involved in this process (Figure 7).

4 | EXPERIMENTAL PROCEDURES

4.1 | Plant materials and growth conditions

For the microarray experiment, Arabidopsis seeds were stratified for 72 h at 4°C and then sown on University of California potting mix type C and vermiculite (3:2 v/v). The plants were grown for 2 weeks (until they had five to six leaves expanded) in a temperature- and humidity-controlled growth chamber under 24°C with 16-h light/21°C with 8-h dark photoperiod providing 180 µmol m^{-2} s^{-1}. For anthocyanin measurements (Figure 4c) and SL treatments (Figure 5c), Arabidopsis seeds were stratified for 72 h at 4°C and then sown on UQ23 potting mix (70% composted pine bark 0–5 mm, 30% coco-peat). Plants were grown for 7 weeks (SL treatments) in temperature- and humidity-controlled growth chambers (16 h:8 h, light:dark, 150 ± 20 µmol m^{-2} s^{-1}, 22°C:20°C, day:night).

4.2 | Treatments for microarray

Two-week-old WT Arabidopsis plants (cv. Colombia-0 or Col-0) were subjected to three different treatments: decapitation (WT_Decap), decapitation + IAA (WT_Decap_IAA), and NPA (WT_NPA) as described in Brewer et al. (2016). Treatments were compared with intact WT and three SL mutants *max1-1*, *max2-1*, and *max3-1* (Booker et al., 2004; Stirnberg et al., 2002). Decapitation involved the removal of the vegetative shoot apex and three to four expanding leaves with scalpel and fine forceps, followed immediately by application of lanolin (<10% EtOH) to the cut surface. For the decapitation + auxin treatment, lanolin was supplemented with 3 mg mL^{-1} of IAA. For NPA treatments, 3 mg ml^{-1} of NPA was applied in a lanolin ring (<10% EtOH) around the top of the hypocotyl. Hypocotyls were collected as three biological replicates of 120–150 plants per treatment or mutant and flash frozen in liquid nitrogen and stored at −80°C. Treatments for each replicate were performed simultaneously, and each biological replicate was harvested over a period of 60–80 min at 24 h after treatment.

4.3 | RNA isolation

Total RNA was isolated using NucleoSpin RNA plant kits (Machery-Nagel, Düren, Germany) and further purified and concentrated using the RNeasy MinElute Cleanup Kit (Qiagen, Hilden, Germany) according to manufacturer's protocol. RNA was quantified using a NanoDrop 1000 Spectrophotometer (Thermo Scientific, Wilmington, Delaware, USA).

4.4 | Microarray hybridization

Hybridization, washing, and scanning were performed at the Clive & Vera Ramaciotti Centre for Gene Function Analysis (University of NSW, Sydney), using Arabidopsis ATH1 genome oligonucleotide chips. High-quality biotin-labeled complementary RNA (cRNA) was prepared from 4-µg total RNA per sample according to the standard Affymetrix protocol, hybridized to whole-genome Arabidopsis ATH1 GeneChips and scanned with an Affymetrix GCS3000 Scanner (Affymetrix, Santa Clara, CA) according to the manufacturer's recommended protocol (GeneChip Expression Analysis Technical Manual).

4.5 | Microarray data pre-processing

The scanned probe array images (.DAT files) were converted into .CEL files using the GeneChip Operating Software (Affymetrix). Affymetrix CEL-data files were preprocessed using the statistical language and environment R version 3.2.2 (Ihaka & Gentleman, 1996). Probe intensities were normalized for background correction using the robust multiarray average method corrected for GC content of the oligo, an algorithm known as GCRMA (Harr & Schlötterer, 2006; Irizarry et al., 2003). GCRMA background correction was used in conjunction with the only perfect match (PM) correction algorithm (Seo & Hoffman, 2006). Gene expression values were calculated from the PM probes using the median polish summary method (Harr & Schlötterer, 2006). Raw gene expression values are supplied in Table S4. The above-mentioned methods were executed using the "affy" (Gautier et al., 2004) and "simpleaffy" (Wilson & Miller, 2005) packages.

4.6 | Microarray data statistical analysis

The limma package (Ritchie et al., 2015; Smyth, 2004) was used to perform moderated *t*-statistics between the treatments to identify DEGs. For each probe, fold change and corresponding *P*-values measuring the statistical significance of DEGs were calculated using empirical Bayesian statistics, which moderates the standard errors within each probe (Ritchie et al., 2015). Benjamini–Hochberg's method was used to correct *P*-values for multiple testing (Benjamini & Hochberg, 1995). We used an adjusted *P*-value (adj *P*-value) cut-off of .05 and absolute LogFC of >2 (|LogFC≥2|) to assign statistical significance. Gene functional annotations obtained from The Arabidopsis Information Resource (TAIR) database (Huala et al., 2001) were used to annotate the genes and match gene IDs to their corresponding probe set numbers provided by the GeneChip manufacturer (Affymetrix).

4.7 | PCA

PCA is a popular multivariate statistical tool that is used to summarize a large number of variables to a smaller number of derived variables that may be readily visualized in two- or three-dimensional space. PCA was applied to summarize and visualize the entire gene expression matrix (all treatment and genes) using the R package "ggfortify" (Tang et al., 2016).

4.8 | Functional enrichment analysis

GO enrichment analysis infers biological meaning from systems biology experiments (Hill et al., 2008). Array IDs of DEGs per comparison against WT_Intact as queries in the DAVID online database for GO enrichment analysis (Dennis et al., 2003). Cytoscape software with the ClueGO package was used to identify and visualize significant ($P < .05$) biological processes represented in each group.

4.9 | Graphs and heatmap rendering

GraphPad Prism 9 or R programming tools for plotting data, "ggplot2" (Wickham, 2016) and "gplots" (Warnes et al., 2009), were used to render graphs and heatmaps.

4.10 | WGCNA

A signed co-expression network was constructed with the WGCNA package in R (Langfelder & Horvath, 2008). WGCNA identifies modules composed of genes that are connected in terms of the topological overlap mapping metric (TOM), a neighborhood proximity measurement that quantifies the degree of sharedness among network neighbors. We used signed network and soft-thresholding power ($\beta = 3$) based on the scale-free model fitting index $R^2 > .9$ (Figure S1A) to obtain an adjacency matrix. The adjacency matrix was transformed into a TOM with the topological overlap (TO)-based dissimilarity (1-TOM). This step resulted in a clustering tree/dendrogram (Figure S1B) whose branches were identified for cutting, depending on their shape. The dynamic tree-cutting algorithm cut the hierarchal clustering tree into modules, that is, clusters of highly co-expressed genes. To obtain moderately large and distinct modules, the default minimum module size was set to 30 genes, and a minimum height for merging modules was .25. Modules were summarized by a hierarchical clustering dendrogram, and module structure was visualized by a heatmap and topological overlap matrix plot. WGCNA assigned to each module a unique color label, and the relationships between each module and treatment/mutants was analyzed to identify the highly correlated modules. Finally, we selected clusters of genes highly correlated with SL biosynthesis and signaling genes and exported them to Cytoscape for network visualization (Shannon et al., 2003).

4.11 | Anthocyanin measurements

For anthocyanin measurements, plants were grown in temperature- and humidity-controlled growth chambers (16 h:8 h, light:dark, 140 ± 10 μmol m^{-2} s^{-1}, 22°C:18°C, day:night). Plants were harvested 5 days before bolting, snap frozen in liquid nitrogen, and ground to a fine powder. To 30–60 mg of powder, 600 μL of 1% HCl in methanol was added and the mixture left overnight at 4°C. The following day, 600 μL of chloroform and 200 μL of water were added. Samples were centrifuged for 10 min at 16,000 x *g*. Anthocyanin content is presented as ($A^{530\ nm}$–$A^{657\ nm}$) per gram of fresh weight.

4.12 | SL treatments

Five microliters of 0- or 5-μM *rac*-GR24 solution in acetone and Tween20 was applied to rosette buds on day 21. Ten microliters was applied on days 24, 32, 35, and 38. On days 27 and 29, 10 μL of 0- or 10-μM GR24 was applied. Branching was scored on day 56, and number of primary rosette branches was normalized by number of leaves.

5 | ACCESSION NUMBERS

AT2G43100, AT5G07690, AT5G09220, AT1G20160, AT2G18550, AT2G22860, AT5G16600, AT5G24420, AT5G15830, AT1G65860, AT1G01110, AT4G25100, AT1G16410, AT1G19670, AT5G23010, AT3G19710, AT3G50970, AT4G15100, AT4G12030, AT2G42610, AT5G59090, AT1G66020, AT4G33420, AT5G38710, AT1G64160, AT5G60020, AT3G22740, AT3G58990, AT1G30760, AT5G25980, AT3G03190, AT4G13770, AT5G64530, AT5G25160, AT1G47400, AT3G21420, AT4G20210, AT1G04240, AT1G04250, AT1G04550, AT1G15580, AT1G17140, AT1G19850, AT1G23080, AT1G28010, AT1G29510, AT1G34670, AT1G48660, AT1G56650, AT1G57560,

AT1G70940, AT1G72430, AT1G73590, AT1G75500, AT1G76520, AT1G77110, AT1G78100, AT2G01940, AT2G16580, AT2G21050, AT2G23170, AT2G26170, AT2G33310, AT2G38120, AT2G44990, AT3G14370, AT3G15540, AT3G28345, AT3G53480, AT3G59900, AT3G62100, AT3G63300, AT4G00880, AT4G14560, AT4G17980, AT4G22620, AT4G27260, AT4G28640, AT4G30290, AT4G32880, AT4G34760, AT4G36110, AT5G13360, AT5G19530, AT5G20820, AT5G39610, AT5G43700, AT5G47370, AT5G54490, AT5G54510, AT5G55250, AT5G62380, AT5G65670, AT5G67480, AT1G03055, AT2G42620, AT3G21420, AT3G03990.

AUTHOR CONTRIBUTIONS

Alicia M. Hellens, Franziska Fichtner, Philip B. Brewer, and Christine A. Beveridge designed the research; Alicia M. Hellens, Franziska Fichtner, and Philip B. Brewer performed the research; Alicia M. Hellens, Tinashe G. Chabikwa, Franziska Fichtner, Philip B. Brewer, and Christine A. Beveridge analyzed the data; Alicia M. Hellens and Tinashe G. Chabikwa wrote the paper. All authors except Tinashe G. Chabikwa edited the manuscript and approved the final version.

ACKNOWLEDGMENTS

Christine Beveridge is the recipient of an Australian Research Council Centre of Excellence CE200100015 and an Australian Laureate Fellowship FL180100139. Alicia Hellens is supported by a Commonwealth Scientific and Industrial Research Organization Postgraduate Scholarship. Philip Brewer is supported by an Australian Research Council Future Fellowship FT180100081. The microarray experiment was performed under the management of Dr. Fiona Filardo and led to the discovery of LATERAL BRANCHING OXIDOREDUCTASE (LBO) in Brewer et al. (2016). The authors are grateful to Dr. François Barbier for helpful comments on the manuscript.

CONFLICT OF INTEREST STATEMENT

The Authors did not report any conflict of interest.

DATA AVAILABILITY STATEMENT

The data that support the findings of this study are openly available in the National Center for Biotechnology Information Gene expression omnibus (NCBI GEO) at https://www.ncbi.nlm.nih.gov/geo/query/acc.cgi?acc=GSE226903 using reference number [GSE226903].

ORCID

Alicia M. Hellens https://orcid.org/0000-0001-9715-8012
Franziska Fichtner https://orcid.org/0000-0002-4508-5437
Philip B. Brewer https://orcid.org/0000-0003-4871-9260
Christine A. Beveridge https://orcid.org/0000-0003-0878-3110

REFERENCES

Abe, S., Sado, A., Tanaka, K., Kisugi, T., Asami, K., Ota, S., Kim, H. I., Yoneyama, K., Xie, X., Ohnishi, T., Seto, Y., Yamaguchi, S., Akiyama, K., Yoneyama, K., & Nomura, T. (2014). Carlactone is converted to carlactonoic acid by MAX1 in Arabidopsis and its methyl ester can directly interact with AtD14 in vitro. *Proceedings of the National Academy of Sciences*, *111*(50), 18084–18089. https://doi.org/10.1073/pnas.1410801111

Agati, G., Azzarello, E., Pollastri, S., & Tattini, M. (2012). Flavonoids as antioxidants in plants: Location and functional significance. *Plant Science*, *196*, 67–76. https://doi.org/10.1016/j.plantsci.2012.07.014

Aguilar-Martínez, J. A., Poza-Carrión, C., & Cubas, P. (2007). Arabidopsis BRANCHED1 acts as an integrator of branching signals within axillary buds. *The Plant Cell*, *19*(2), 458–472. https://doi.org/10.1105/tpc.106.048934

Alder, A., Jamil, M., Marzorati, M., Bruno, M., Vermathen, M., Bigler, P., Ghisla, S., Bouwmeester, H., Beyer, P., & Al-Babili, S. (2012). The path from β-carotene to carlactone, a strigolactone-like plant hormone. *Science (New York, N.Y.)*, *335*(6074), 1348–1351. https://doi.org/10.1126/science.1218094

Araki, R., Hasumi, A., Nishizawa, O. I., Sasaki, K., Kuwahara, A., Sawada, Y., Totoki, Y., Toyoda, A., Sakaki, Y., Li, Y., Saito, K., Ogawa, T., & Hirai, M. Y. (2013). Novel bioresources for studies of Brassica oleracea: Identification of a kale MYB transcription factor responsible for glucosinolate production. *Plant Biotechnology Journal*, *11*(8), 1017–1027. https://doi.org/10.1111/pbi.12095

Arite, T., Umehara, M., Ishikawa, S., Hanada, A., Maekawa, M., Yamaguchi, S., & Kyozuka, J. (2009). d14, a strigolactone-insensitive mutant of rice, shows an accelerated outgrowth of tillers. *Plant and Cell Physiology*, *50*(8), 1416–1424. https://doi.org/10.1093/pcp/pcp091

Ashburner, M., Ball, C. A., Blake, J. A., Botstein, D., Butler, H., Cherry, J. M., Davis, A. P., Dolinski, K., Dwight, S. S., Eppig, J. T., Harris, M. A., Hill, D. P., Issel-Tarver, L., Kasarskis, A., Lewis, S., Matese, J. C., Richardson, J. E., Ringwald, M., Rubin, G. M., & Sherlock, G. (2000). Gene ontology: Tool for the unification of biology. *Nature Genetics*, *25*(1), 25–29. https://doi.org/10.1038/75556

Augustine, R., & Bisht, N. C. (2017). Regulation of glucosinolate metabolism: From model plant Arabidopsis thaliana to Brassica crops. In J.-M. Mérillon & K. G. Ramawat (Eds.), *Glucosinolates*. Reference Series in Phytochemistry. (pp. 163–199). Springer International Publishing. https://doi.org/10.1007/978-3-319-25462-3_3

Bainbridge, K., Sorefan, K., Ward, S., & Leyser, O. (2005). Hormonally controlled expression of the Arabidopsis MAX4 shoot branching regulatory gene. *The Plant Journal*, *44*(4), 569–580. https://doi.org/10.1111/j.1365-313X.2005.02548.x

Bak, S., & Feyereisen, R. (2001). The involvement of two P450 enzymes, CYP83B1 and CYP83A1, in auxin homeostasis and glucosinolate biosynthesis. *Plant Physiology*, *127*(1), 108–118. https://doi.org/10.1104/pp.127.1.108

Barbier, F. F., Cao, D., Fichtner, F., Weiste, C., Perez-Garcia, M. D., Caradeuc, M., le Gourrierec, J., Sakr, S., & Beveridge, C. A. (2021). HEXOKINASE1 signalling promotes shoot branching and interacts with cytokinin and strigolactone pathways. *New Phytologist*, *231*, 1088–1104. https://doi.org/10.1111/nph.17427

Barbier, F. F., Dun, E. A., Kerr, S. C., Chabikwa, T. G., & Beveridge, C. A. (2019). An update on the signals controlling shoot branching. *Trends in Plant Science*, *24*(3), 220–236. https://doi.org/10.1016/j.tplants.2018.12.001

Barbier, F. F., Lunn, J. E., & Beveridge, C. A. (2015). Ready, steady, go! A sugar hit starts the race to shoot branching. *Current Opinion in Plant Biology*, *25*, 39–45. https://doi.org/10.1016/j.pbi.2015.04.004

Barbier, F. F., Péron, T., Lecerf, M., Perez-Garcia, M. D., Barrière, Q., Rolčík, J., Boutet-Mercey, S., Citerne, S., Lemoine, R., Porcheron, B., Roman, H., Leduc, N., le Gourrierec, J., Bertheloot, J., & Sakr, S. (2015). Sucrose is an early modulator of the key hormonal mechanisms controlling bud outgrowth in Rosa hybrida. *Journal of Experimental Botany*, *66*(9), 2569–2582. https://doi.org/10.1093/jxb/erv047

Benjamini, Y., & Hochberg, Y. (1995). Controlling the false discovery rate: A practical and powerful approach to multiple testing. *Journal of the Royal Statistical Society: Series B: Methodological*, *57*(1), 289–300. https://doi.org/10.1111/j.2517-6161.1995.tb02031.x

Bennett, T., Sieberer, T., Willett, B., Booker, J., Luschnig, C., & Leyser, O. (2006). The Arabidopsis MAX pathway controls shoot branching by regulating auxin transport. *Current Biology*, *16*(6), 553–563. https://doi.org/10.1016/j.cub.2006.01.058

Bertheloot, J., Barbier, F., Boudon, F., Perez-Garcia, M. D., Péron, T., Citerne, S., Dun, E., Beveridge, C., Godin, C., & Sakr, S. (2020). Sugar availability suppresses the auxin-induced strigolactone pathway to promote bud outgrowth. *New Phytologist*, *225*(2), 866–879. https://doi.org/10.1111/nph.16201

Beveridge, C. A. (2000). Long-distance signalling and a mutational analysis of branching in pea. *Plant Growth Regulation*, *32*(2), 193–203. https://doi.org/10.1023/A:1010718020095

Booker, J., Auldridge, M., Wills, S., McCarty, D., Klee, H., & Leyser, O. (2004). MAX3/CCD7 is a carotenoid cleavage dioxygenase required for the synthesis of a novel plant signaling molecule. *Current Biology*, *14*(14), 1232–1238. https://doi.org/10.1016/j.cub.2004.06.061

Bouwmeester, H. J., Roux, C., Lopez-Raez, J. A., & Bécard, G. (2007). Rhizosphere communication of plants, parasitic plants and AM fungi. *Trends in Plant Science*, *12*(5), 224–230. https://doi.org/10.1016/j.tplants.2007.03.009

Braun, N., de Saint Germain, A., Pillot, J. P., Boutet-Mercey, S., Dalmais, M., Antoniadi, I., Li, X., Maia-Grondard, A., le Signor, C., Bouteiller, N., Luo, D., Bendahmane, A., Turnbull, C., & Rameau, C. (2012). The pea TCP transcription factor PsBRC1 acts downstream of strigolactones to control shoot branching1[W]. *Plant Physiology*, *158*(1), 225–238. https://doi.org/10.1104/pp.111.182725

Bressan, M., Roncato, M. A., Bellvert, F., Comte, G., Haichar, F. Z., Achouak, W., & Berge, O. (2009). Exogenous glucosinolate produced by Arabidopsis thaliana has an impact on microbes in the rhizosphere and plant roots. *The ISME Journal*, *3*(11), 1243–1257. https://doi.org/10.1038/ismej.2009.68

Brewer, P. B., Dun, E. A., Ferguson, B. J., Rameau, C., & Beveridge, C. A. (2009). Strigolactone acts downstream of auxin to regulate bud outgrowth in pea and Arabidopsis. *Plant Physiology*, *150*(1), 482–493. https://doi.org/10.1104/pp.108.134783

Brewer, P. B., Koltai, H., & Beveridge, C. A. (2013). Diverse roles of strigolactones in plant development. *Molecular Plant*, *6*(1), 18–28. https://doi.org/10.1093/mp/sss130

Brewer, P. B., Yoneyama, K., Filardo, F., Meyers, E., Scaffidi, A., Frickey, T., Akiyama, K., Seto, Y., Dun, E. A., Cremer, J. E., Kerr, S. C., Waters, M. T., Flematti, G. R., Mason, M. G., Weiller, G., Yamaguchi, S., Nomura, T., Smith, S. M., Yoneyama, K., & Beveridge, C. A. (2016). LATERAL BRANCHING OXIDOREDUCTASE acts in the final stages of strigolactone biosynthesis in Arabidopsis. *Proceedings of the National Academy of Sciences*, *113*(22), 6301–6306. https://doi.org/10.1073/pnas.1601729113

Bürger, M., & Chory, J. (2020). The many models of strigolactone signaling. *Trends in Plant Science*, *25*(4), 395–405. https://doi.org/10.1016/j.tplants.2019.12.009

Burow, M., Atwell, S., Francisco, M., Kerwin, R. E., Halkier, B. A., & Kliebenstein, D. J. (2015). The glucosinolate biosynthetic gene AOP2 mediates feed-back regulation of jasmonic acid signaling in Arabidopsis. *Molecular Plant*, *8*(8), 1201–1212. https://doi.org/10.1016/j.molp.2015.03.001

Burow, M., & Halkier, B. A. (2017). How does a plant orchestrate defense in time and space? Using glucosinolates in Arabidopsis as case study. *Current Opinion in Plant Biology*, *38*, 142–147. https://doi.org/10.1016/j.pbi.2017.04.009

Bursch, K., Niemann, E. T., Nelson, D. C., & Johansson, H. (2021). Karrikins control seedling photomorphogenesis and anthocyanin biosynthesis through a HY5-BBX transcriptional module. *The Plant Journal*, *107*(5), 1346–1362. https://doi.org/10.1111/tpj.15383

Chen, S., Glawischnig, E., Jørgensen, K., Naur, P., Jørgensen, B., Olsen, C. E., Hansen, C. H., Rasmussen, H., Pickett, J. A., & Halkier, B. A. (2003). CYP79F1 and CYP79F2 have distinct functions in the biosynthesis of aliphatic glucosinolates in Arabidopsis. *The Plant Journal*, *33*(5), 923–937. https://doi.org/10.1046/j.1365-313X.2003.01679.x

Chevalier, F., Nieminen, K., Sánchez-Ferrero, J. C., Rodríguez, M. L., Chagoyen, M., Hardtke, C. S., & Cubas, P. (2014). Strigolactone promotes degradation of DWARF14, an α/β hydrolase essential for strigolactone signaling in Arabidopsis. *The Plant Cell*, *26*(3), 1134–1150. https://doi.org/10.1105/tpc.114.122903

Chew, F. S. (1988). Biological effects of glucosinolates. In *Biologically active natural products* (pp. 155–181). American Chemical Society. https://doi.org/10.1021/bk-1988-0380.ch012

Cline, M. G. (1996). Exogenous auxin effects on lateral bud outgrowth in decapitated shoots. *Annals of Botany*, *78*(2), 255–266. https://doi.org/10.1006/anbo.1996.0119

Cook, C. E., Whichard, L. P., Wall, M. E., Egley, G. H., Coggon, P., Luhan, P. A., & McPhail, A. T. (1972). Germination stimulants. II. Structure of strigol, a potent seed germination stimulant for witchweed (Striga lutea). *Journal of the American Chemical Society*, *94*(17), 6198–6199. https://doi.org/10.1021/ja00772a048

Crawford, S., Shinohara, N., Sieberer, T., Williamson, L., George, G., Hepworth, J., Müller, D., Domagalska, M. A., & Leyser, O. (2010). Strigolactones enhance competition between shoot branches by dampening auxin transport. *Development (Cambridge, England)*, *137*(17), 2905–2913. https://doi.org/10.1242/dev.051987

Das, P. K., Shin, D. H., Choi, S. B., & Park, Y. I. (2012). Sugar-hormone cross-talk in anthocyanin biosynthesis. *Molecules and Cells*, *34*(6), 501–507. https://doi.org/10.1007/s10059-012-0151-x

Deikman, J., & Hammer, P. E. (1995). Induction of anthocyanin accumulation by cytokinins in Arabidopsis thaliana. *Plant Physiology*, *108*(1), 47–57. https://doi.org/10.1104/pp.108.1.47

Dennis, G., Sherman, B. T., Hosack, D. A., Yang, J., Gao, W., Lane, H. C., & Lempicki, R. A. (2003). DAVID: Database for Annotation, Visualization, and Integrated Discovery. *Genome Biology*, *4*(9), R60. https://doi.org/10.1186/gb-2003-4-9-r60

Dun, E. A., de Saint Germain, A., Rameau, C., & Beveridge, C. A. (2012). Antagonistic action of strigolactone and cytokinin in bud outgrowth control. *Plant Physiology*, *158*(1), 487–498. https://doi.org/10.1104/pp.111.186783

Eisen, M. B., Spellman, P. T., Brown, P. O., & Botstein, D. (1998). Cluster analysis and display of genome-wide expression patterns. *Proceedings of the National Academy of Sciences*, *95*(25), 14863–14868. https://doi.org/10.1073/pnas.95.25.14863

Faizan, M., Faraz, A., Sami, F., Siddiqui, H., Yusuf, M., Gruszka, D., & Hayat, S. (2020). Role of strigolactones: Signalling and crosstalk with other phytohormones. *Open Life Sciences*, *15*(1), 217–228. https://doi.org/10.1515/biol-2020-0022

Fernández, I., Cosme, M., Stringlis, I. A., Yu, K., Jonge, R., van Wees, S. C. M., Pozo, M. J., Pieterse, C. M. J., & van der Heijden, M. G. A. (2019). Molecular dialogue between arbuscular mycorrhizal fungi and the nonhost plant Arabidopsis thaliana switches from initial detection to antagonism. *New Phytologist*, *223*(2), 867–881. https://doi.org/10.1111/nph.15798

Ferrero, M., Pagliarani, C., Novák, O., Ferrandino, A., Cardinale, F., Visentin, I., & Schubert, A. (2018). Exogenous strigolactone interacts with abscisic acid-mediated accumulation of anthocyanins in grapevine berries. *Journal of Experimental Botany*, *69*(9), 2391–2401. https://doi.org/10.1093/jxb/ery033

Fichtner, F., Barbier, F. F., Annunziata, M. G., Feil, R., Olas, J. J., Mueller-Roeber, B., Stitt, M., Beveridge, C. A., & Lunn, J. E. (2021).

Regulation of shoot branching in Arabidopsis by trehalose 6-phosphate. *New Phytologist*, *229*(4), 2135–2151. https://doi.org/10.1111/nph.17006

Fichtner, F., Barbier, F. F., Feil, R., Watanabe, M., Annunziata, M. G., Chabikwa, T. G., Höfgen, R., Stitt, M., Beveridge, C. A., & Lunn, J. E. (2017). Trehalose 6-phosphate is involved in triggering axillary bud outgrowth in garden pea (Pisum sativum L.). *The Plant Journal: For Cell and Molecular Biology*, *92*(4), 611–623. https://doi.org/10.1111/tpj.13705

Fichtner, F., & Lunn, J. E. (2021). The role of trehalose 6-phosphate (Tre6P) in plant metabolism and development. *Annual Review of Plant Biology*, *72*(1), 737–760. https://doi.org/10.1146/annurev-arplant-050718-095929

Foo, E., Bullier, E., Goussot, M., Foucher, F., Rameau, C., & Beveridge, C. A. (2005). The branching gene RAMOSUS1 mediates interactions among two novel signals and auxin in pea. *The Plant Cell*, *17*(2), 464–474. https://doi.org/10.1105/tpc.104.026716

Francisco, M., Joseph, B., Caligagan, H., Li, B., Corwin, J. A., Lin, C., Kerwin, R., Burow, M., & Kliebenstein, D. J. (2016). The defense metabolite, allyl glucosinolate, modulates Arabidopsis thaliana biomass dependent upon the endogenous glucosinolate pathway. *Frontiers in Plant Science*, *7*, 774. https://doi.org/10.3389/fpls.2016.00774

Gautier, L., Cope, L., Bolstad, B. M., & Irizarry, R. A. (2004). Affy—Analysis of Affymetrix GeneChip data at the probe level. *Bioinformatics*, *20*(3), 307–315. https://doi.org/10.1093/bioinformatics/btg405

Gendreau, E., Traas, J., Desnos, T., Grandjean, O., Caboche, M., & Hofte, H. (1997). Cellular basis of hypocotyl growth in Arabidopsis thaliana. *Plant Physiology*, *114*(1), 295–305. https://doi.org/10.1104/pp.114.1.295

Gigolashvili, T., Yatusevich, R., Rollwitz, I., Humphry, M., Gershenzon, J., & Flügge, U. I. (2009). The plastidic bile acid transporter 5 is required for the biosynthesis of methionine-derived glucosinolates in Arabidopsis thaliana. *The Plant Cell*, *21*(6), 1813–1829. https://doi.org/10.1105/tpc.109.066399

Gomez-Roldan, V., Fermas, S., Brewer, P. B., Puech-Pagès, V., Dun, E. A., Pillot, J. P., Letisse, F., Matusova, R., Danoun, S., Portais, J. C., Bouwmeester, H., Bécard, G., Beveridge, C. A., Rameau, C., & Rochange, S. F. (2008). Strigolactone inhibition of shoot branching. *Nature*, *455*(7210), 189–194. https://doi.org/10.1038/nature07271

González-Grandío, E., Pajoro, A., Franco-Zorrilla, J. M., Tarancón, C., Immink, R. G., & Cubas, P. (2017). Abscisic acid signaling is controlled by a BRANCHED1/HD-ZIP I cascade in Arabidopsis axillary buds. *Proceedings of the National Academy of Sciences*, *114*(2), E245–E254. https://doi.org/10.1073/pnas.1613199114

Gould, K. S., McKelvie, J., & Markham, K. R. (2002). Do anthocyanins function as antioxidants in leaves? Imaging of H2O2 in red and green leaves after mechanical injury. *Plant, Cell & Environment*, *25*(10), 1261–1269. https://doi.org/10.1046/j.1365-3040.2002.00905.x

Ha, C. V., Leyva-González, M. A., Osakabe, Y., Tran, U. T., Nishiyama, R., Watanabe, Y., Tanaka, M., Seki, M., Yamaguchi, S., Dong, N. V., Yamaguchi-Shinozaki, K., Shinozaki, K., Herrera-Estrella, L., & Tran, L. S. (2014). Positive regulatory role of strigolactone in plant responses to drought and salt stress. *Proceedings of the National Academy of Sciences of the United States of America*, *111*, 851–856. https://doi.org/10.1073/pnas.1322135111

Halkier, B. A., & Gershenzon, J. (2006). Biology and biochemistry of glucosinolates. *Annual Review of Plant Biology*, *57*(1), 303–333. https://doi.org/10.1146/annurev.arplant.57.032905.105228

Hamiaux, C., Drummond, R. S. M., Janssen, B. J., Ledger, S. E., Cooney, J. M., Newcomb, R. D., & Snowden, K. C. (2012). DAD2 is an α/β Hydrolase likely to be involved in the perception of the plant branching hormone, strigolactone. *Current Biology*, *22*(21), 2032–2036. https://doi.org/10.1016/j.cub.2012.08.007

Hansen, C. H., Wittstock, U., Olsen, C. E., Hick, A. J., Pickett, J. A., & Halkier, B. A. (2001). Cytochrome P450 CYP79F1 from Arabidopsis catalyzes the conversion of dihomomethionine and trihomomethionine to the corresponding aldoximes in the biosynthesis of aliphatic glucosinolates*. *Journal of Biological Chemistry*, *276*(14), 11078–11085. https://doi.org/10.1074/jbc.M010123200

Harr, B., & Schlötterer, C. (2006). Comparison of algorithms for the analysis of Affymetrix microarray data as evaluated by co-expression of genes in known operons. *Nucleic Acids Research*, *34*(2), e8–e8. https://doi.org/10.1093/nar/gnj010

Hayward, A., Stirnberg, P., Beveridge, C., & Leyser, O. (2009). Interactions between auxin and strigolactone in shoot branching control. *Plant Physiology*, *151*(1), 400–412. https://doi.org/10.1104/pp.109.137646

Hill, D. P., Smith, B., McAndrews-Hill, M. S., & Blake, J. A. (2008). Gene ontology annotations: What they mean and where they come from. *BMC Bioinformatics*, *9*(Suppl 5), S2. https://doi.org/10.1186/1471-2105-9-S5-S2

Hruz, T., Laule, O., Szabo, G., Wessendorp, F., Bleuler, S., Oertle, L., Widmayer, P., Gruissem, W., & Zimmermann, P. (2008). Genevestigator V3: A reference expression database for the meta-analysis of transcriptomes. *Advances in Bioinformatics*, *2008*, 420747. https://doi.org/10.1155/2008/420747

Huala, E., Dickerman, A. W., Garcia-Hernandez, M., Weems, D., Reiser, L., LaFond, F., Hanley, D., Kiphart, D., Zhuang, M., Huang, W., Mueller, L. A., Bhattacharyya, D., Bhaya, D., Sobral, B. W., Beavis, W., Meinke, D. W., Town, C. D., Somerville, C., & Rhee, S. Y. (2001). The Arabidopsis information resource (TAIR): A comprehensive database and web-based information retrieval, analysis, and visualization system for a model plant. *Nucleic Acids Research*, *29*(1), 102–105. https://doi.org/10.1093/nar/29.1.102

Huang, D. W., Sherman, B. T., & Lempicki, R. A. (2009). Systematic and integrative analysis of large gene lists using DAVID bioinformatics resources. *Nature Protocols*, *4*(1), 44–57. https://doi.org/10.1038/nprot.2008.211

Ihaka, R., & Gentleman, R. (1996). R: A language for data analysis and graphics. *Journal of Computational and Graphical Statistics*, *5*(3), 299–314. https://doi.org/10.1080/10618600.1996.10474713

Irizarry, R. A., Bolstad, B. M., Collin, F., Cope, L. M., Hobbs, B., & Speed, T. P. (2003). Summaries of Affymetrix GeneChip probe level data. *Nucleic Acids Research*, *31*(4), e15–e15, 115. https://doi.org/10.1093/nar/gng015

Ishikawa, S., Maekawa, M., Arite, T., Onishi, K., Takamure, I., & Kyozuka, J. (2005). Suppression of tiller bud activity in tillering dwarf mutants of rice. *Plant and Cell Physiology*, *46*(1), 79–86. https://doi.org/10.1093/pcp/pci022

Ito, S., Nozoye, T., Sasaki, E., Imai, M., Shiwa, Y., Shibata-Hatta, M., Ishige, T., Fukui, K., Ito, K., Nakanishi, H., Nishizawa, N. K., Yajima, S., & Asami, T. (2015). Strigolactone regulates anthocyanin accumulation, acid phosphatases production and plant growth under low phosphate condition in Arabidopsis. *PLoS ONE*, *10*(3), e0119724. https://doi.org/10.1371/journal.pone.0119724

Ji, X.-H., Wang, Y. T., Zhang, R., Wu, S. J., An, M. M., Li, M., Wang, C. Z., Chen, X. L., Zhang, Y. M., & Chen, X. S. (2015). Effect of auxin, cytokinin and nitrogen on anthocyanin biosynthesis in callus cultures of red-fleshed apple (Malus sieversii f.niedzwetzkyana). *Plant Cell, Tissue and Organ Culture (PCTOC)*, *120*(1), 325–337. https://doi.org/10.1007/s11240-014-0609-y

Kebrom, T. H. (2017). A growing stem inhibits bud outgrowth—The overlooked theory of apical dominance. *Frontiers in Plant Science*, *8*, 1874. https://doi.org/10.3389/fpls.2017.01874

Kelly, J. H., Tucker, M. R., & Brewer, P. B. (2023). The strigolactone pathway is a target for modifying crop shoot architecture and yield. *Biology*, *12*(1), 95. https://doi.org/10.3390/biology12010095

Klepikova, A. V., Kasianov, A. S., Gerasimov, E. S., Logacheva, M. D., & Penin, A. A. (2016). A high resolution map of the Arabidopsis thaliana developmental transcriptome based on RNA-seq profiling. *The Plant Journal*, *88*(6), 1058–1070. https://doi.org/10.1111/tpj.13312

Kruckelmann, H. W. (1975). Effect of fertilizers, soils, soil tillage, and plant species on the frequency of endogone chlamydospores and mycorrhizal infection in arable soils. In F. E. Sanders, B. Mosse, & P. B. Tinker (Eds.), *Endomycorrhizas, Proceedings of a Symposium held at the University of Leeds, 22–25 July 1974*. Academic Press.

Kumar, M., Kim, I., Kim, Y. K., Heo, J. B., Suh, M. C., & Kim, H. U. (2019). Strigolactone signaling genes showing differential expression patterns in Arabidopsis max mutants. *Plants*, *8*(9), 352. https://doi.org/10.3390/plants8090352

Landi, M., Tattini, M., & Gould, K. S. (2015). Multiple functional roles of anthocyanins in plant-environment interactions. *Environmental and Experimental Botany*, *119*, 4–17. https://doi.org/10.1016/j.envexpbot.2015.05.012

Lanfranco, L., Fiorilli, V., Venice, F., & Bonfante, P. (2018). Strigolactones cross the kingdoms: Plants, fungi, and bacteria in the arbuscular mycorrhizal symbiosis. *Journal of Experimental Botany*, *69*(9), 2175–2188. https://doi.org/10.1093/jxb/erx432

Langfelder, P., & Horvath, S. (2008). WGCNA: An R package for weighted correlation network analysis. *BMC Bioinformatics*, *9*(1), 559. https://doi.org/10.1186/1471-2105-9-559

Lantzouni, O., Klermund, C., & Schwechheimer, C. (2017). Largely additive effects of gibberellin and strigolactone on gene expression in Arabidopsis thaliana seedlings. *The Plant Journal*, *92*(5), 924–938. https://doi.org/10.1111/tpj.13729

Li, B., Gaudinier, A., Tang, M., Taylor-Teeples, M., Nham, N. T., Ghaffari, C., Benson, D. S., Steinmann, M., Gray, J. A., Brady, S. M., & Kliebenstein, D. J. (2014). Promoter-based integration in plant defense regulation. *Plant Physiology*, *166*(4), 1803–1820. https://doi.org/10.1104/pp.114.248716

Li, B., Tang, M., Nelson, A., Caligagan, H., Zhou, X., Clark-Wiest, C., Ngo, R., Brady, S. M., & Kliebenstein, D. J. (2018). Network-guided discovery of extensive epistasis between transcription factors involved in aliphatic glucosinolate biosynthesis. *The Plant Cell*, *30*(1), 178–195. https://doi.org/10.1105/tpc.17.00805

Ligerot, Y., de Saint Germain, A., Waldie, T., Troadec, C., Citerne, S., Kadakia, N., Pillot, J. P., Prigge, M., Aubert, G., Bendahmane, A., Leyser, O., Estelle, M., Debellé, F., & Rameau, C. (2017). The pea branching RMS2 gene encodes the PsAFB4/5 auxin receptor and is involved in an auxin-strigolactone regulation loop. *PLoS Genetics*, *13*(12), e1007089. https://doi.org/10.1371/journal.pgen.1007089

Liu, Y., Tikunov, Y., Schouten, R. E., Marcelis, L. F. M., Visser, R. G. F., & Bovy, A. (2018). Anthocyanin biosynthesis and degradation mechanisms in solanaceous vegetables: A review. *Frontiers in Chemistry*, *6*, 52. https://doi.org/10.3389/fchem.2018.00052

Liu, Z., Shi, M.-Z., & Xie, D.-Y. (2014). Regulation of anthocyanin biosynthesis in Arabidopsis thaliana red pap1-D cells metabolically programmed by auxins. *Planta*, *239*(4), 765–781. https://doi.org/10.1007/s00425-013-2011-0

Marcotte, E. M., Pellegrini, M., Thompson, M. J., Yeates, T. O., & Eisenberg, D. (1999). A combined algorithm for genome-wide prediction of protein function. *Nature*, *402*(6757), 83–86. https://doi.org/10.1038/47048

Mashiguchi, K., Sasaki, E., Shimada, Y., Nagae, M., Ueno, K., Nakano, T., Yoneyama, K., Suzuki, Y., & Asami, T. (2009). Feedback-regulation of strigolactone biosynthetic genes and strigolactone-regulated genes in Arabidopsis. *Bioscience, Biotechnology, and Biochemistry*, *73*(11), 2460–2465. https://doi.org/10.1271/bbb.90443

Mashiguchi, K., Seto, Y., Onozuka, Y., Suzuki, S., Takemoto, K., Wang, Y., Dong, L., Asami, K., Noda, R., Kisugi, T., Kitaoka, N., Akiyama, K., Bouwmeester, H., & Yamaguchi, S. (2022). A carlactonoic acid methyltransferase that contributes to the inhibition of shoot branching in Arabidopsis. *Proceedings of the National Academy of Sciences of the United States of America*, *119*, e2111565119. https://doi.org/10.1073/pnas.2111565119

Mason, M. G., Ross, J. J., Babst, B. A., Wienclaw, B. N., & Beveridge, C. A. (2014). Sugar demand, not auxin, is the initial regulator of apical dominance. *Proceedings of the National Academy of Sciences of the United States of America*, *111*, 6092–6097. https://doi.org/10.1073/pnas.1322045111

Nelson, D. C., Scaffidi, A., Dun, E. A., Waters, M. T., Flematti, G. R., Dixon, K. W., Beveridge, C. A., Ghisalberti, E. L., & Smith, S. M. (2011). F-box protein MAX2 has dual roles in karrikin and strigolactone signaling in Arabidopsis thaliana. *Proceedings of the National Academy of Sciences*, *108*(21), 8897–8902. https://doi.org/10.1073/pnas.1100987108

Ozeki, Y., & Komamine, A. (1986). Effects of growth regulators on the induction of anthocyanin synthesis in carrot suspension cultures. *Plant and Cell Physiology*, *27*(7), 1361–1368. https://doi.org/10.1093/oxfordjournals.pcp.a077234

Pandey, A., Sharma, M., & Pandey, G. K. (2016). Emerging roles of strigolactones in plant responses to stress and development. *Frontiers in Plant Science*, *7*. https://doi.org/10.3389/fpls.2016.00434

Patil, S. B., Barbier, F. F., Zhao, J., Zafar, S. A., Uzair, M., Sun, Y., Fang, J., Perez-Garcia, M. D., Bertheloot, J., Sakr, S., Fichtner, F., Chabikwa, T. G., Yuan, S., Beveridge, C. A., & Li, X. (2021). Sucrose promotes D53 accumulation and tillering in rice. *New Phytologist*, *234*, 122–136. https://doi.org/10.1111/nph.17834

Reintanz, B., Lehnen, M., Reichelt, M., Gershenzon, J., Kowalczyk, M., Sandberg, G., Godde, M., Uhl, R., & Palme, K. (2001). Bus, a bushy Arabidopsis CYP79F1 knockout mutant with abolished synthesis of short-chain aliphatic glucosinolates. *The Plant Cell*, *13*(2), 351–367. https://doi.org/10.1105/tpc.13.2.351

Richmond, B. L., Coelho, C. L., Wilkinson, H., McKenna, J., Ratchinski, P., Schwarze, M., Frost, M., Lagunas, B., & Gifford, M. L. (2022). Elucidating connections between the strigolactone biosynthesis pathway, flavonoid production and root system architecture in Arabidopsis thaliana. *Physiologia Plantarum*, *174*(2), e13681. https://doi.org/10.1111/ppl.13681

Ritchie, M. E., Phipson, B., Wu, D., Hu, Y., Law, C. W., Shi, W., & Smyth, G. K. (2015). limma powers differential expression analyses for RNA-sequencing and microarray studies. *Nucleic Acids Research*, *43*(7), e47–e47. https://doi.org/10.1093/nar/gkv007

Robert-Seilaniantz, A., Grant, M., & Jones, J. D. G. (2011). Hormone crosstalk in plant disease and defense: More than just JASMONATE-SALICYLATE antagonism. *Annual Review of Phytopathology*, *49*(1), 317–343. https://doi.org/10.1146/annurev-phyto-073009-114447

Saeed, W., Naseem, S., & Ali, Z. (2017). Strigolactones biosynthesis and their role in abiotic stress resilience in plants: A critical review. *Frontiers in Plant Science*, *8*, 1487. Available at: https://www.frontiersin.org/article/10.3389/fpls.2017.01487 (Accessed: 23 February 2022)

Salehin, M., Li, B., Tang, M., Katz, E., Song, L., Ecker, J. R., Kliebenstein, D. J., & Estelle, M. (2019). Auxin-sensitive Aux/IAA proteins mediate drought tolerance in Arabidopsis by regulating glucosinolate levels. *Nature Communications*, *10*(1), 4021. https://doi.org/10.1038/s41467-019-12002-1

Seo, J., & Hoffman, E. P. (2006). Probe set algorithms: Is there a rational best bet? *BMC Bioinformatics*, *7*(1), 395. https://doi.org/10.1186/1471-2105-7-395

Seto, Y., Sado, A., Asami, K., Hanada, A., Umehara, M., Akiyama, K., & Yamaguchi, S. (2014). Carlactone is an endogenous biosynthetic precursor for strigolactones. *Proceedings of the National Academy of Sciences*, *111*(4), 1640–1645. https://doi.org/10.1073/pnas.1314805111

Shannon, P., Markiel, A., Ozier, O., Baliga, N. S., Wang, J. T., Ramage, D., Amin, N., Schwikowski, B., & Ideker, T. (2003). Cytoscape: A software environment for integrated models of biomolecular interaction

networks. *Genome Research*, *13*(11), 2498–2504. https://doi.org/10.1101/gr.1239303

Shen, H., Zhu, L., Bu, Q. Y., & Huq, E. (2012). MAX2 affects multiple hormones to promote photomorphogenesis. *Molecular Plant*, *5*(3), 750–762. https://doi.org/10.1093/mp/sss029

Shinohara, N., Taylor, C., & Leyser, O. (2013). Strigolactone can promote or inhibit shoot branching by triggering rapid depletion of the auxin efflux protein PIN1 from the plasma membrane. *PLoS Biology*, *11*(1), e1001474. https://doi.org/10.1371/journal.pbio.1001474

Smith, S. M., & Li, J. (2014). Signalling and responses to strigolactones and karrikins. *Current Opinion in Plant Biology*, *21*, 23–29. https://doi.org/10.1016/j.pbi.2014.06.003

Smyth, G. K. (2004). Linear models and empirical bayes methods for assessing differential expression in microarray experiments. *Statistical Applications in Genetics and Molecular Biology*, *3*, 3. https://doi.org/10.2202/1544-6115.1027

Sønderby, I. E., Geu-Flores, F., & Halkier, B. A. (2010). Biosynthesis of glucosinolates–gene discovery and beyond. *Trends in Plant Science*, *15*(5), 283–290. https://doi.org/10.1016/j.tplants.2010.02.005

Soundappan, I., Bennett, T., Morffy, N., Liang, Y., Stanga, J. P., Abbas, A., Leyser, O., & Nelson, D. C. (2015). SMAX1-LIKE/D53 family members enable distinct MAX2-dependent responses to Strigolactones and karrikins in Arabidopsis. *The Plant Cell*, *27*(11), 3143–3159. https://doi.org/10.1105/tpc.15.00562

Stirnberg, P., Furner, I. J., & Leyser, H. M. O. (2007). MAX2 participates in an SCF complex which acts locally at the node to suppress shoot branching. *The Plant Journal*, *50*(1), 80–94. https://doi.org/10.1111/j.1365-313X.2007.03032.x

Stirnberg, P., van de Sande, K., & Leyser, H. M. O. (2002). MAX1 and MAX2 control shoot lateral branching in Arabidopsis. *Development*, *129*(5), 1131–1141. https://doi.org/10.1242/dev.129.5.1131

Tanaka, Y., Sasaki, N., & Ohmiya, A. (2008). Biosynthesis of plant pigments: Anthocyanins, betalains and carotenoids. *The Plant Journal*, *54*(4), 733–749. https://doi.org/10.1111/j.1365-313X.2008.03447.x

Tang, Y., Horikoshi, M., & Li, W. (2016). ggfortify: Unified interface to visualize statistical results of popular R packages. *The R Journal*, *8*(2), 474. https://doi.org/10.32614/RJ-2016-060

Tantikanjana, T., Mikkelsen, M. D., Hussain, M., Halkier, B. A., & Sundaresan, V. (2004). Functional analysis of the tandem-duplicated P450 genes SPS/BUS/CYP79F1 and CYP79F2 in glucosinolate biosynthesis and plant development by Ds transposition-generated double mutants. *Plant Physiology*, *135*(2), 840–848. https://doi.org/10.1104/pp.104.040113

Tantikanjana, T., Yong, J. W. H., Letham, D. S., Griffith, M., Hussain, M., Ljung, K., Sandberg, G., & Sundaresan, V. (2001). Control of axillary bud initiation and shoot architecture in Arabidopsis through the SUPERSHOOT gene. *Genes & Development*, *15*(12), 1577–1588. https://doi.org/10.1101/gad.887301

Teng, S., Keurentjes, J., Bentsink, L., Koornneef, M., & Smeekens, S. (2005). Sucrose-specific induction of anthocyanin biosynthesis in Arabidopsis requires the MYB75/PAP1 gene. *Plant Physiology*, *139*(4), 1840–1852. https://doi.org/10.1104/pp.105.066688

Umehara, M., Hanada, A., Yoshida, S., Akiyama, K., Arite, T., Takeda-Kamiya, N., Magome, H., Kamiya, Y., Shirasu, K., Yoneyama, K., Kyozuka, J., & Yamaguchi, S. (2008). Inhibition of shoot branching by new terpenoid plant hormones. *Nature*, *455*(7210), 195–200. https://doi.org/10.1038/nature07272

Wakabayashi, T., Yasuhara, R., Miura, K., Takikawa, H., Mizutani, M., & Sugimoto, Y. (2021). Specific methylation of (11R)-carlactonoic acid by an Arabidopsis SABATH methyltransferase. *Planta*, *254*(5), 88. https://doi.org/10.1007/s00425-021-03738-6

Wang, L., Wang, B., Jiang, L., Liu, X., Li, X., Lu, Z., Meng, X., Wang, Y., Smith, S. M., & Li, J. (2015). 'Strigolactone signaling in Arabidopsis regulates shoot development by targeting D53-like SMXL repressor proteins for ubiquitination and degradation. *Report*, *27*(11), 3128–3142. https://doi.org/10.1105/tpc.15.00605

Wang, L., Wang, B., Yu, H., Guo, H., Lin, T., Kou, L., Wang, A., Shao, N., Ma, H., Xiong, G., Li, X., Yang, J., Chu, J., & Li, J. (2020). Transcriptional regulation of strigolactone signalling in Arabidopsis. *Nature*, *583*(7815), 277–281. https://doi.org/10.1038/s41586-020-2382-x

Wang, Y., Sun, J., Wang, N., Xu, H., Qu, C., Jiang, S., Fang, H., Su, M., Zhang, Z., & Chen, X. (2019). MdMYBL2 helps regulate cytokinin-induced anthocyanin biosynthesis in red-fleshed apple (Malus sieversii f. niedzwetzkyana) callus. *Functional Plant Biology*, *46*(2), 187–196. https://doi.org/10.1071/FP17216

Warnes, G. R., Bolker, B., Bonebakker, L., Gentleman, R., Huber, W., Liaw, A., Lumley, T., Maechler, M., Magnusson, A., Moeller, S., & Schwartz, M. (2009). gplots: Various R programming tools for plotting data. *R Package Version*, *2*(4), 1.

Waters, M. T., Brewer, P. B., Bussell, J. D., Smith, S. M., & Beveridge, C. A. (2012). The Arabidopsis ortholog of rice DWARF27 acts upstream of MAX1 in the control of plant development by strigolactones. *Plant Physiology*, *159*(3), 1073–1085. https://doi.org/10.1104/pp.112.196253

Waters, M. T., Nelson, D. C., Scaffidi, A., Flematti, G. R., Sun, Y. K., Dixon, K. W., & Smith, S. M. (2012). Specialisation within the DWARF14 protein family confers distinct responses to karrikins and strigolactones in Arabidopsis. *Development*, *139*(7), 1285–1295. https://doi.org/10.1242/dev.074567

Weijers, D., & Wagner, D. (2016). Transcriptional responses to the auxin hormone. *Annual Review of Plant Biology*, *67*(1), 539–574. https://doi.org/10.1146/annurev-arplant-043015-112122

Whipple, C. J., Kebrom, T. H., Weber, A. L., Yang, F., Hall, D., Meeley, R., Schmidt, R., Doebley, J., Brutnell, T. P., & Jackson, D. P. (2011). Grassy tillers1 promotes apical dominance in maize and responds to shade signals in the grasses. *Proceedings of the National Academy of Sciences*, *108*(33), E506–E512. https://doi.org/10.1073/pnas.1102819108

Wickham, H. (2016). Programming with ggplot2. In H. Wickham (Ed.), *ggplot2: Elegant graphics for data analysis* (pp. 241–253). Springer International Publishing (Use R!). https://doi.org/10.1007/978-3-319-24277-4_12

Wilson, C. L., & Miller, C. J. (2005). Simpleaffy: A BioConductor package for Affymetrix quality control and data analysis. *Bioinformatics*, *21*(18), 3683–3685. https://doi.org/10.1093/bioinformatics/bti605

Winter, D., Vinegar, B., Nahal, H., Ammar, R., Wilson, G. V., & Provart, N. J. (2007). An "electronic fluorescent pictograph" browser for exploring and analyzing large-scale biological data sets. *PLoS ONE*, *2*(8), e718. https://doi.org/10.1371/journal.pone.0000718

Xu, E., Chai, L., Zhang, S., Yu, R., Zhang, X., Xu, C., & Hu, Y. (2021). Catabolism of strigolactones by a carboxylesterase. *Nature Plants*, *7*(11), 1495–1504. https://doi.org/10.1038/s41477-021-01011-y

Yoneyama, K., & Brewer, P. B. (2021). Strigolactones, how are they synthesized to regulate plant growth and development? *Current Opinion in Plant Biology*, *63*, 102072. https://doi.org/10.1016/j.pbi.2021.102072

Yoneyama, K., Kisugi, T., Xie, X., Arakawa, R., Ezawa, T., Nomura, T., & Yoneyama, K. (2015). Shoot-derived signals other than auxin are involved in systemic regulation of strigolactone production in roots. *Planta*, *241*(3), 687–698. https://doi.org/10.1007/s00425-014-2208-x

Young, N. F., Ferguson, B. J., Antoniadi, I., Bennett, M. H., Beveridge, C. A., & Turnbull, C. G. N. (2014). Conditional auxin response and differential cytokinin profiles in shoot branching mutants. *Plant Physiology*, *165*(4), 1723–1736. https://doi.org/10.1104/pp.114.239996

Zhang, X., Ivanova, A., Vandepoele, K., Radomiljac, J., van de Velde, J., Berkowitz, O., Willems, P., Xu, Y., Ng, S., van Aken, O., Duncan, O., Zhang, B., Storme, V., Chan, K. X., Vaneechoutte, D., Pogson, B. J., van Breusegem, F., Whelan, J., & de Clercq, I. (2017). The transcription factor MYB29 is a regulator of ALTERNATIVE OXIDASE1a. *Plant Physiology*, *173*(3), 1824–1843. https://doi.org/10.1104/pp.16.01494

Zhang, J., Mazur, E., Balla, J., Gallei, M., Kalousek, P., Medveďová, Z., Li, Y., Wang, Y., Prát, T., Vasileva, M., Reinöhl, V., Procházka, S., Halouzka, R., Tarkowski, P., Luschnig, C., Brewer, P. B., & Friml, J. (2020). Strigolactones inhibit auxin feedback on PIN-dependent auxin transport canalization. *Nature Communications*, *11*(1). https://doi.org/10.1038/s41467-020-17252-y

Zhao, Y., Christensen, S. K., Fankhauser, C., Cashman, J. R., Cohen, J. D., Weigel, D., & Chory, J. (2001). A role for flavin monooxygenase-like enzymes in auxin biosynthesis. *Science* [Preprint], *291*, 306–309. https://doi.org/10.1126/science.291.5502.306

Zheng, X. T., Yu, Z. C., Tang, J. W., Cai, M. L., Chen, Y. L., Yang, C. W., Chow, W. S., & Peng, C. L. (2020). The major photoprotective role of anthocyanins in leaves of Arabidopsis thaliana under long-term high light treatment: Antioxidant or light attenuator? *Photosynthesis Research* [Preprint], *149*, 25–40. https://doi.org/10.1007/s11120-020-00761-8

Zuluaga, D. L., Graham, N. S., Klinder, A., van Ommen Kloeke, A. E. E., Marcotrigiano, A. R., Wagstaff, C., Verkerk, R., Sonnante, G., & Aarts, M. G. M. (2019). Overexpression of the MYB29 transcription factor affects aliphatic glucosinolate synthesis in Brassica oleracea. *Plant Molecular Biology*, *101*(1–2), 65–79. https://doi.org/10.1007/s11103-019-00890-2

SUPPORTING INFORMATION

Additional supporting information can be found online in the Supporting Information section at the end of this article.

How to cite this article: Hellens, A. M., Chabikwa, T. G., Fichtner, F., Brewer, P. B., & Beveridge, C. A. (2023). Identification of new potential downstream transcriptional targets of the strigolactone pathway including glucosinolate biosynthesis. *Plant Direct*, *7*(3), e486. https://doi.org/10.1002/pld3.486